714
ORNL-4956

PREPARATION, TESTING, AND ANALYSIS OF ZINC DIFFUSION SAMPLES NASA SKYLAB EXPERIMENT M-558

D. N. Braski
E. H. Kobisk
F. R. O'Donnell

OAK RIDGE NATIONAL LABORATORY
OPERATED BY UNION CARBIDE CORPORATION • FOR THE U.S. ATOMIC ENERGY COMMISSION

Printed in the United States of America. Available from
National Technical Information Service
U.S. Department of Commerce
5285 Port Royal Road, Springfield, Virginia 22151
Price: Printed Copy $5.45; Microfiche $1.45

ORNL-4956
UC-4 Chemistry

Contract No. W-7405-eng-26

ISOTOPES DEVELOPMENT CENTER

PREPARATION, TESTING, AND ANALYSIS OF ZINC DIFFUSION SAMPLES NASA SKYLAB EXPERIMENT M-558

D. N. Braski, E. H. Kobisk, and F. R. O'Donnell

Isotopes Division

APRIL 1974

OAK RIDGE NATIONAL LABORATORY
Oak Ridge, Tennessee 37830
operated by
UNION CARBIDE CORPORATION
for the
U.S. ATOMIC ENERGY COMMISSION

CONTENTS

PREPARATION, TESTING, AND ANALYSIS OF ZINC DIFFUSION SAMPLES NASA SKYLAB EXPERIMENT M-558

D. N. Braski, E. H. Kobisk, and F. R. O'Donnell

SUMMARY

Transport mechanisms of zinc atoms in molten zinc were investigated by radiotracer techniques in unit and in near-zero gravity environments. This project was proposed by Dr. Anthony O. Ukanwa of the NASA Marshall Space Flight Center as an experiment for the Skylab program. Preparation of ground test and flight samples together with subsequent analysis of the zinc radioisotope distribution within each sample before and after fusion was performed by personnel of the ORNL Isotopes Division, Isotope Research Materials Laboratory.

The purpose of these various experiments was to determine the relative roles of convection and diffusion in the transport of ^{65}Zn (and therefore normal zinc) from a well-defined region within a zinc bar during melting and as a function of time in the molten state. Each melt in the Skylab flight experiments was maintained in a thermal gradient of 420°C to 790°C. Similar tests were performed in a unit gravity environment for comparison.

Each zinc sample was encased in a graphite capsule and finally in a tantalum capsule welded closed to achieve a leak-tight seal. Samples were subjected to vibration, acceleration, and shock tests at the Westinghouse Astronuclear Laboratories and experienced no failure. Roughly one quarter of the total zinc bar was pre-irradiated in a thermal neutron field to activate the normal zinc to attain a ^{65}Zn concentration of ∿20 μCi. This portion was then joined to unactivated pure zinc either at the end of the bar or in the midsection of the bar. Experimental assembly in the gradient furnace was such that one sample had its radioactive zone located in the 420°C region, one sample was reversed so that the active zone was in the 790°C end and, finally, the third sample was midway in the gradient zone.

After melting in the gradient furnace followed by a thermal soak period (the latter was used for flight samples only), the samples were cooled and analyzed for ^{65}Zn distribution. All samples melted in a unit gravity environment were found to have uniform ^{65}Zn distribution — no concentration gradient was observed even when the sample was brought rapidly to melting and then quenched. Space-melted samples, however, showed "textbook" distributions, obviously the result of diffusion. It was evident that convection phenomena were the dominant

factors influencing zinc transport in unit gravity experiments, while simple diffusion was the dominant factor in near-zero gravity experiments.

Zinc-65 distribution was determined by precise machining of the samples with subsequent gamma counting of each machined piece. Concentration data were obtained both in the axial direction and in the radial direction. This technique was found to be highly accurate and proved that the use of radioisotope tracers can be a valuable tool in performing space experimentation, where applicable. Deleterious effects of radiation in the vicinity of stored experimental samples aboard the space craft were found to be insignificant even when photographic film cassettes were placed in close proximity to the samples. Over-all, this entire experiment was totally successful with respect to obtaining significant information on the use of radioisotope tracers in space and especially concerning the differences between operating transport mechanisms in liquid metals in space and in a unit gravity environment.

Data treatment, calculations, and theoretical conclusions resulting from this experiment (and other Skylab experiments) can be found in the collection of information to be published by NASA (no reference available at this time).

INTRODUCTION

At the request of NASA (Marshall Space Flight Center) personnel, services of the Isotopes Research Materials Laboratory, Isotopes Division, were provided in the fabrication, radioisotope tagging, testing, and final data accumulation for the NASA Skylab Experiment M-558. The experiment was performed on NASA Skylab-III and was designed to investigate diffusion and convection phenomena in a thermal gradient and in a near-zero gravitational environment. The principal investigator for this experiment was Dr. Anthony O. Ukanwa (NASA).

Oak Ridge National Laboratory personnel were responsible for fabrication of the zinc samples, appropriate radioisotope tracer preparation, encapsulation of the zinc samples in tantalum and graphite shells, performance of selected ground tests, and tracer analysis of the final distribution of radioisotope zinc after both ground-based and flight experiments. Precision sectioning of the bars after fusion and cooling was used to obtain samples from which the concentration gradient of ^{65}Zn could be determined by radiation counting. Subsequent data analysis and computation of diffusion and convection kinetics were performed by Dr. Ukanwa and other NASA personnel; these data are not presented, but can be found in the NASA Skylab journals to be published in the near future (reference unknown).

MATERIALS

Materials used to fabricate the M-558 specimen hardware include high-purity zinc, ATJ carbon, tantalum tubing, and tantalum bar. The vendors and chemical analyses for these materials are listed in Appendix A.

SAMPLE FABRICATION

Zinc Bar Specimens

Zinc bar specimens were fabricated from 1/2-in.-diam ingots which were subsequently cold drawn into bars of 5/16-in. diameter. The bars were machined to a $0.286\ ^{+0.000}_{-0.001}$ in. diam and cut into 1.592-, 0.796-, and 0.250-in. lengths. These pieces were used to construct the bar specimens of two different configurations as shown in Fig. 1. One 1.592-in.-long bar bonded to a 0.250-in. pellet on one end was called an A-type specimen (Fig. 1a), while two 0.796-in.-long bars bonded to a 0.250-in. pellet in the center comprised a B-type specimen (Fig. 1b). The final length of both A- and B-type specimens was $1.842\ ^{+0.000}_{-0.002}$ in. However, before the machined bars were bonded, all the mating surfaces were polished to a mirror finish and the 0.250-in. pellets, which serve as the source of ^{65}Zn tracer material, were irradiated in a reactor.

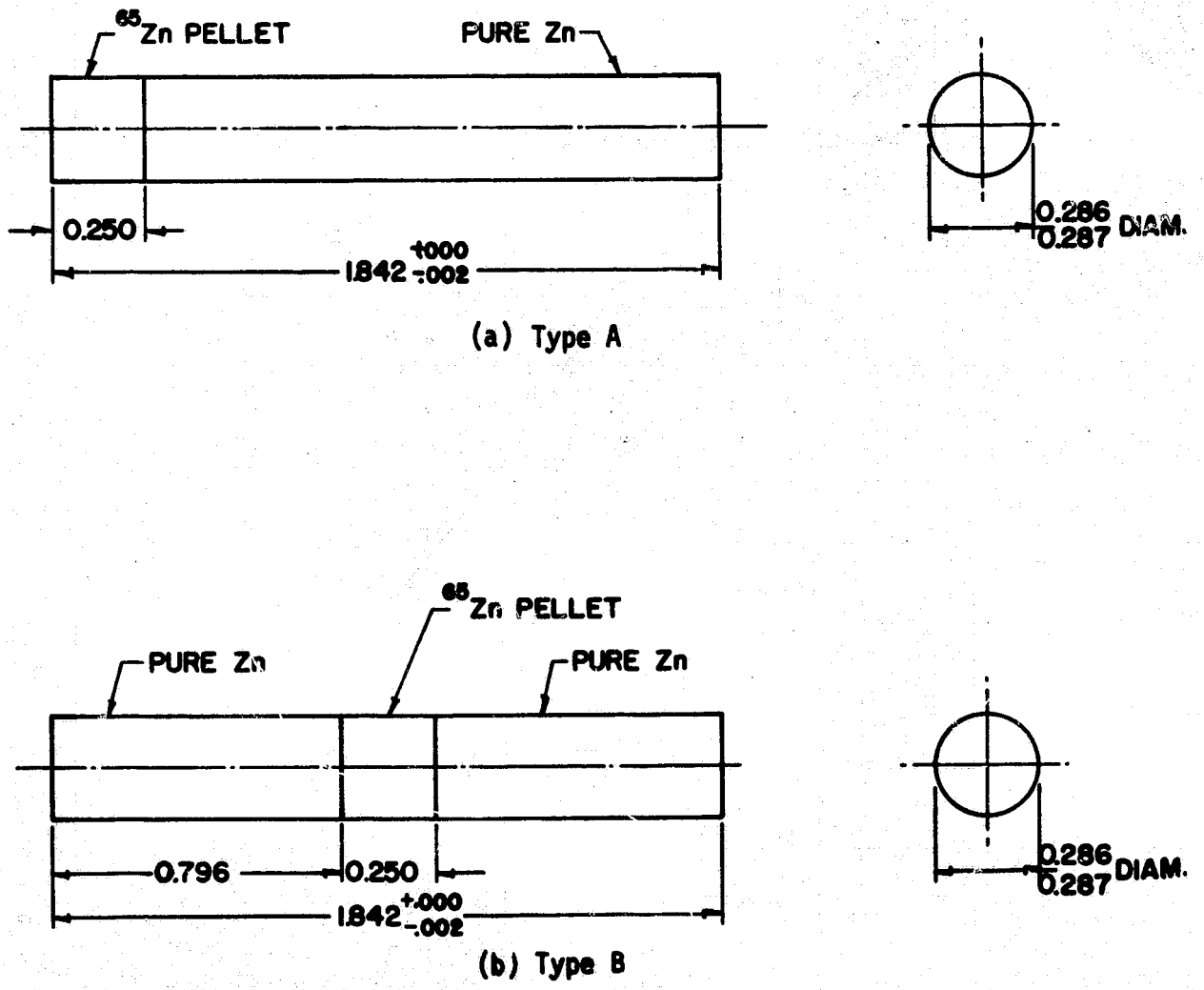

Fig. 1. Zinc-65 Tracer Specimens.

Polishing Zinc Surfaces

Since cold welding was to be used to join the bars and pellets, it was imperative that the mating surfaces be as flat, smooth, and clean as possible. To accomplish this, the bars and pellets were mounted in epoxy and wet ground by hand through number 600 emery paper. After a thorough washing, the samples were then polished on a vibratory polisher using pellon cloth and a 0.3-micron aluminum oxide polishing compound. The pellets for the B-type specimens (Fig. 1b) were ground and polished on two parallel surfaces. The bars and pellets were then removed from their epoxy mounts by dissolution of the epoxy in Hysol solvent (a proprietary epoxy solvent), washed in distilled water, rinsed in absolute ethyl alcohol, and dried in warm air.

Irradiation of Zinc Pellets

All of the 0.250-in. pellets were irradiated in the Bulk Shielding Reactor (BSR) at ORNL on October 5, 1972. They were placed in either the S-3 or N-4 tubes for 90 min and subjected to a flux of 1.5×10^2 n/cm^2·sec thermal neutrons and a fluence of 7.0×10^7 n/cm^2·sec fast neutrons. The irradiation produced ^{65}Zn in the pellets to an activity level of approximately 20 μCi per pellet. Zinc-65 decays to ^{65}Cu by two branches as shown schematically in Fig. 2.[1] Slightly over half of the ^{65}Zn decay (50.6%) involves an electron-capture process to an excited ^{65}Cu* state at 1.1155 MeV. Decay of the ^{65}Cu* to stable ^{65}Cu produces gamma radiation of 1.1155-MeV energy. The other branch involves electron capture (48.0%) and positron (β_1^+) emission (1.4%) with a 0.331-MeV energy as decay occurs directly to the stable ^{65}Cu. The electron capture also leads to subsequent atomic reactions producing x rays and Auger electrons. The half-life for ^{65}Zn decay is 243.8 days.

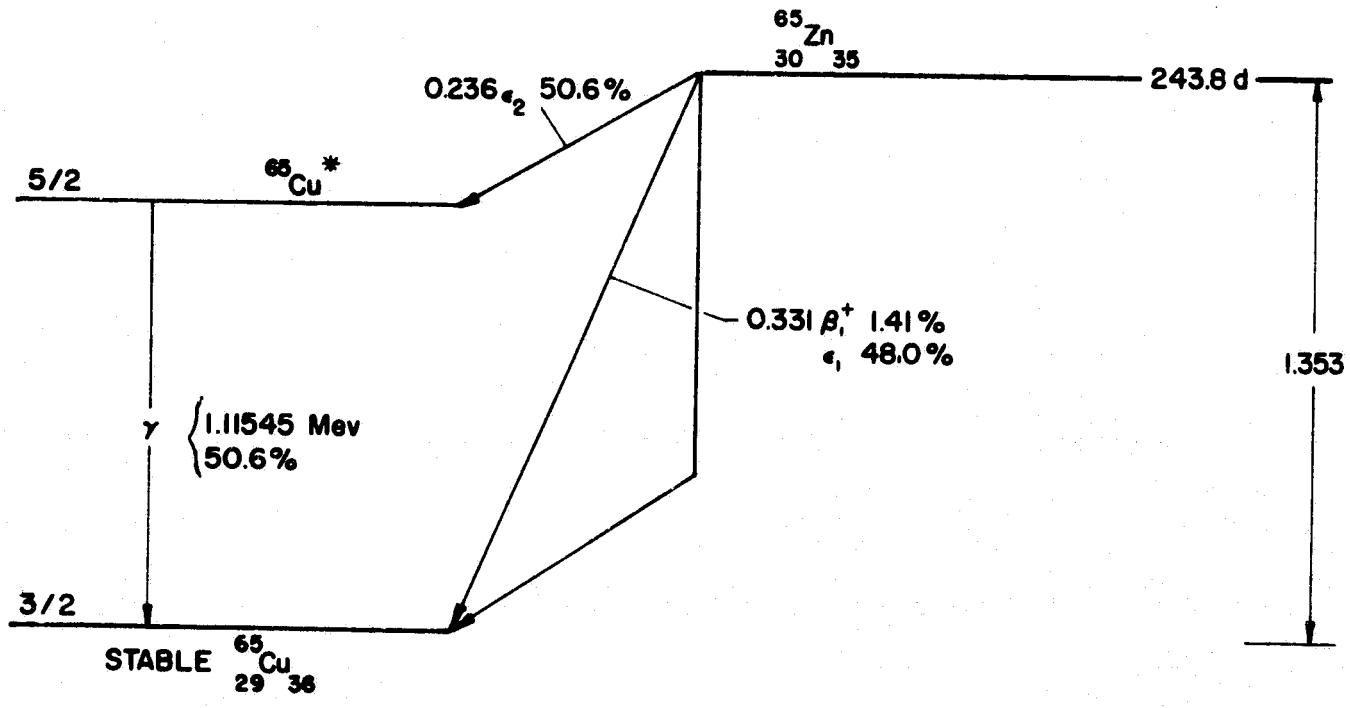

Fig. 2. Zinc-65 Decay Scheme.

[1]M. J. Martin and P. Blichert-Toft, *Nuclear Data Tables*, Vol. 8, No. 1-2, Academic Press, October 1970.

Joining Zinc Specimens

After investigating numerous joining techniques, a method of cold-welding the ^{65}Zn tracer pellets to the unirradiated zinc bar(s) (see Fig. 1) was developed. The equipment needed to conduct the process included a 5-ton capacity hydraulic press and a hardened steel die with a 0.286-in.-diam ram as shown in Fig. 3. To join A-type specimens (Fig. 1a), the mating surfaces of a 1.592-in.-long bar and ^{65}Zn pellet were first lightly abraded on 600-grit emery paper. The two pieces were then etched for 1 to 2 min in an acid solution containing one part concentrated HCl and three parts distilled water. The zinc bar was then inserted in the die on top of the bottom ram with the abraded surface facing upwards. A drop of the acid solution was placed on this surface. The ^{65}Zn pellet was then inserted in the die, followed by the upper ram, and the entire assembly was placed in the hydraulic press. A load of 1500 to 1700 lb (23,400 to 26,600 psi in compression at the zinc interface) was sufficient to produce a cold-weld bond between the zinc bar and ^{65}Zn pellet. However, this force also caused substantial plastic flow of the zinc in the die body making removal of the bonded specimen difficult. Loads of 2000 lb or more were sometimes needed to eject the specimens which invariably resulted in specimen breakage. This problem was solved by immersing the die in a cold bath of dry ice and acetone for 5 min. Since the thermal contraction of zinc was twice that of the steel die, it was possible to eject the zinc specimen with loads of 100 lb or less, and specimen failure seldom occurred. It should be pointed out that this entire procedure was carried out using techniques and a special hood designed for handling radioactive materials. The purpose for using acid in the joining process was to dissolve the oxide film from the interface, thus permitting cold-welding of two clean surfaces. The acid itself was not incorporated into the zinc specimen, but was forced out of the interface at low compressive load. Continued loading forced the zinc to expand and fill the die cavity which in turn expelled the acid from the die along paths between the zinc specimen and die walls. The B-type specimens were joined in a similar manner, except that two bonding operations were needed. First a ^{65}Zn pellet was bonded to a 0.796-in.-long zinc bar (see Fig. 1b) and ejected after cooling the die in the dry ice–acetone bath. Then the remaining surface of the ^{65}Zn was lightly abraded on 600-grit emery paper and the entire sample was etched in the hydrochloric acid solution (1 HCl:3 H_2O) for 2 to 4 min. Extra etching was

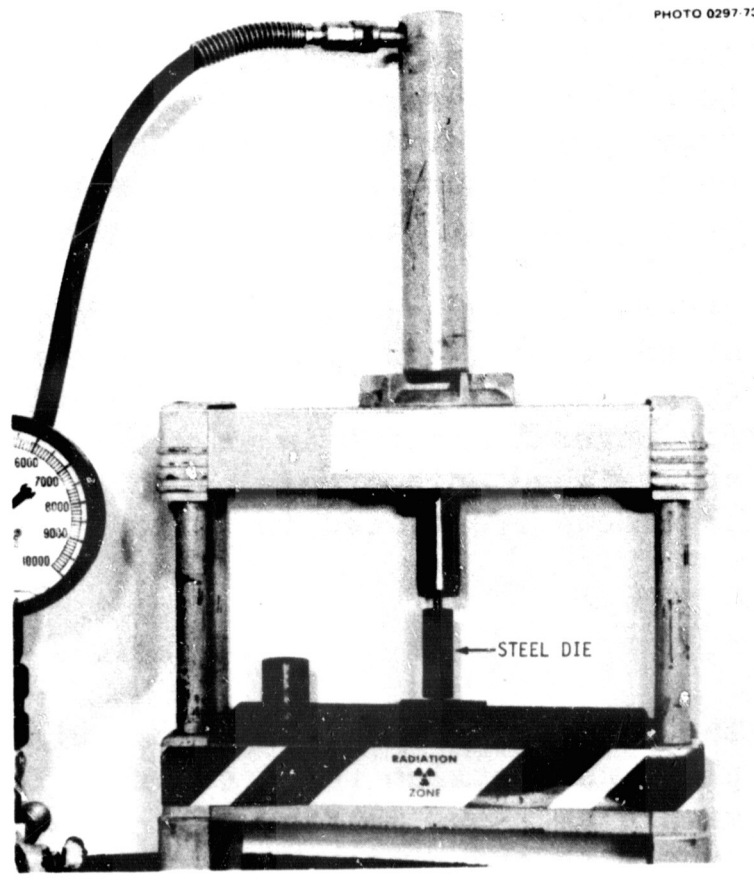

Fig. 3. Hydraulic Press and Steel Die Used to Join Zinc Specimens.

sometimes needed to reduce the diameter of the zinc specimen so that it could be easily reinserted into the die. Finally, the second 0.796-in.-long zinc bar was bonded to the other half with the ^{65}Zn pellet using a load of 1700 to 1900 lb. The increased pressure needed to form the second bond was necessary to compensate for the increased sample hardness resulting from work hardening during the first pressing. Moreover, if the second bond failed upon ejection from the die, it was necessary to repeat the second bonding procedure using a 1900- to 2100-lb load.

After the zinc specimens were joined, they were rinsed in methyl alcohol, dried in air, and chemically cleaned for 15 sec in a solution containing 40 g Cr_2O_3, 3 g Na_2SO_4, and 200 ml H_2O. The specimens were then rinsed for several minutes in an ultrasonic bath of methyl alcohol, dried in air, and weighed on a precision Mettler microbalance. The weights of the zinc specimens are listed in Table 1.

Capsule Fabrication

The components of a flight capsule consisted of two solid tantalum end plugs, a tantalum tube, a carbon tube, two carbon end caps, and the zinc sample as shown in Fig. 4a. The zinc sample was placed in the carbon tube with end caps, which, in turn, was fitted inside the tantalum tube. The tantalum end plugs were welded in argon to the tantalum tube, producing a sealed sample capsule. The capsules were permanently labeled at one end by vibratory engraving according to the scheme depicted in Figs. 4b and 4c. The first letter on the label was either an "A" or "B" and defined the type of zinc sample contained. Type "A" capsules followed by an even number (0, 2, 4, etc.) had the sample oriented with the ^{65}Zn pellet near the labeled end (Fig. 4b), while type "A" capsules followed by odd numbers (1, 3, 5, etc.) had the ^{65}Zn pellet oriented away from the labeled end (Fig. 4c). Flight instructions stated that the capsules would be placed in the gradient furnace such that their labeled ends were located in the colder zone of the furnace.

Cleaning

The carbon tubes and end caps were cleaned by heating at 850°C for 1-1/2 hr under a hydrogen atmosphere. Tantalum tubes and end plugs were degreased for 15 min in an ultrasonic bath containing trichloroethylene, followed by a 15-min rinse in an ultrasonic bath of ethyl alcohol. The cleaning treatment for the zinc sample was described in the previous section.

Welding

The tantalum capsules were welded manually by the tungsten-inert-gas (TIG) process in an inert gas glove box. Capsules were loaded into the glove box and fixed vertically in a mechanical chuck, which was mounted to a motorized turntable to allow rotation of the specimen. Copper chill blocks were placed around the tantalum tube to help dissipate heat from the welding

TABLE 1. Zinc Cylinder Data

Capsule No.	Zn Wt. (Before Melting) (g)	Zn Wt. (After Melting) (g)	Pellet Bond As Shown By Radiograph	Facility where Radiographed	Cylinder Length After Melting (in.)	Cylinder Diameter After Melting (in.)	Cylinder Activity After Melting (μCi/g)	Date Activity Measured
A0	13.6432	13.6344	Good	Westinghouse	1.685	0.298	22.77	12-21-72
A1	13.5587	13.5589	Good	Westinghouse	1.682	0.299	20.28	12-21-72
A2	13.6180		Good	Westinghouse	1.668	0.299	19.72*	12-7-72
A3	13.5991		Good	Westinghouse	1.690	0.299	20.11*	12-5-72
A4	13.5424		Good	Westinghouse				
A5	13.5912		Good	Westinghouse				
A6	13.5846		Good	Westinghouse				
A7	13.6367		Good	Westinghouse				
A8	13.6374		Good	Westinghouse				
A9	13.6321		Good	Westinghouse				
A11	13.6151		Not radiog.	-				
A12	13.5710		Not radiog.	-				
A13	13.6581		Not radiog.	-	1.685	0.300	17.27*	12-13-72
A14	13.6508		Not radiog.	-	1.766	0.300	19.30	12-12-72
A15	13.6459	13.6447	Not radiog.	-	1.740	0.300	19.10	1-12-73
A16	13.5934		Not radiog.	-				
B1	13.5062		1 bond bad	Westinghouse				
B2	13.5550		Good	Westinghouse				
B3	13.4750		1 bond bad	Westinghouse				
B4	13.3376		2 bonds bad	Westinghouse				
B5	13.5613		1 bond bad	Westinghouse				
B6**	12.8628		Not radiog.	-				
B7	13.4406		Not radiog.	-				
B8	13.2752		Not radiog.	-				
B9	13.2883		2 bonds bad	ORNL				
B10***	13.0460		1 bond bad	ORNL			19.90	11-30-72
B11	13.3983		1 bond bad	ORNL				
B12	13.5559		Good	ORNL				
B13	13.3009	13.3002	Good	ORNL	1.646	0.300	18.63	12-21-72
B14	13.3336		Good	ORNL				
B15	13.4275		Good	ORNL				

*Calculated by adding the activities of all the sections and the activity of lost material.
**Used in preliminary melt test. Broke at both bonds during melt.
***Zinc-65 pellet used for decay determination.

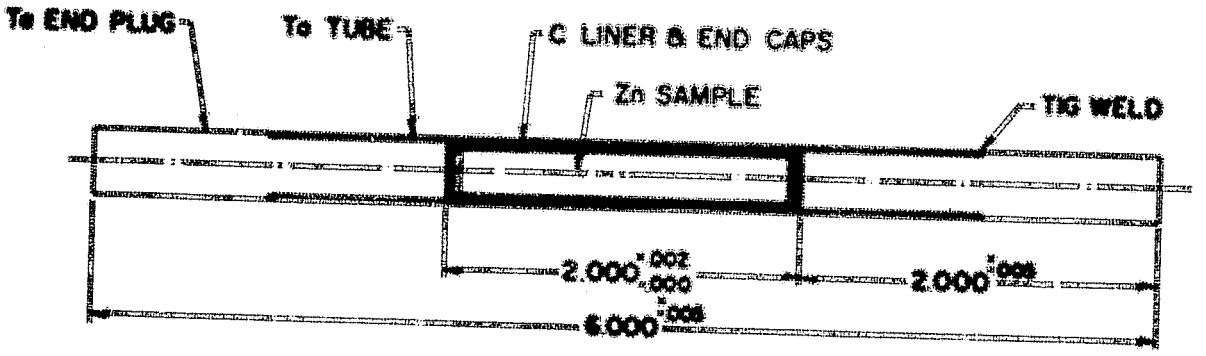

(a) Tantalum Capsule

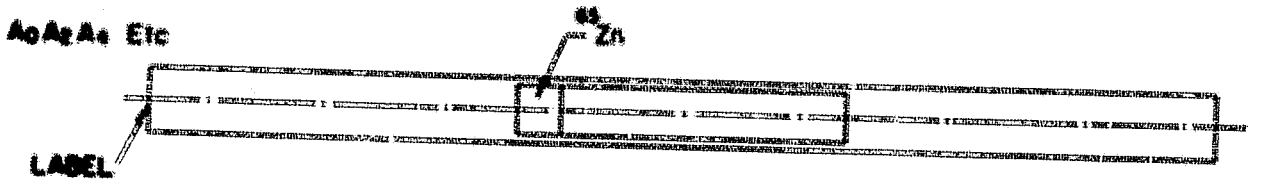

(b) "A(even)" Type Capsules

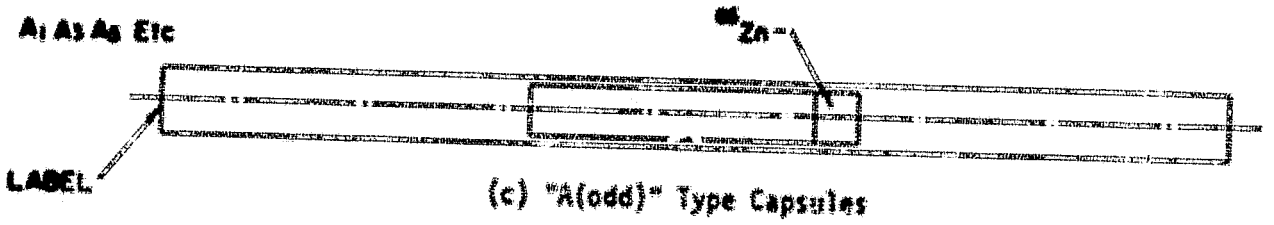

(c) "A(odd)" Type Capsules

Fig. 4. Tantalum Capsule Fabrication and Labeling Scheme.

process. The glove box was then evacuated to 5×10^{-6} Torr and back-filled with argon. Both tantalum end caps were subsequently TIG-welded at conditions of approximately 12 V and 100 A dc using pure tantalum filler wire. The weld metal was subsequently centerless ground flush with the tube and end caps.

Leak Checking Tantalum Capsules

Welded capsules were leak tested by immersion in a bath of ethylene glycol at approximately 100°C. Emission of tiny bubbles from any spot on the capsule indicated the presence and location of leaks in the capsule. Several capsules were found to have leaks in the weld zone and were rewelded. Subsequent leak tests showed the repaired capsules to be hermetically sealed.

X-Ray Radiographs of Tantalum Capsules

Seven B-type capsules, B-9 through B-15, were radiographed to check the bond lines. This test was initiated after the specimens in capsules B-1, B-3, B-4, and B-5 of the original five flight sets were found to exhibit suspicious or faulty bond lines as shown by x-ray radiography. All of the A-type specimens and sample B-2 were satisfactory. X-ray radiographs were taken at ORNL with a Norelco 300 x-ray unit at 300 kV and 10 mA for 2 min, using a tube-to-object distance of 55 in. Since the radiographs showed that capsules B-12, B-13, B-14, and B-15 contained zinc specimens with satisfactory bonds, these capsules were substituted in the flight sets for capsules B-1, B-3, B-4, and B-5 (see Table 2).

TABLE 2

Flight Sets and Ground Test Capsules

1. Capsules sent to Westinghouse 10-13-72

Flight Set	Capsule Numbers
I	A-0, A-1, B-1
II	A-2, A-3, B-2
III	A-4, A-5, B-3
IV	A-6, A-7, B-4
V	A-8, A-9, B-5

2. Revised sets due to substitution of B-1, B-3, B-4, B-5, with B-12, B-13, B-14, and B-15 sent to Westinghouse 10-31-72

Flight Set	Capsule Numbers
I	A-0*, A-1*, B-13*
II	A-2*, A-3*, B-14*
III	A-4, A-5, B-15
IV	A-6, A-7, B-2
V	A-8, A-9, B-12

3. Ground Test Capsules (ORNL)

A-11*, A-13*, A-15*
A-12*, A-14*, A-16
B-1, B-3, B-4, B-5, B-6*, B-7*, B-8*, B-9, B-10*, B-11

*Capsule has been involved in a ground test as of 1-31-73.

GROUND TESTS

The capsules that were allocated for ground tests at ORNL as well as those of the sets that were tested at the Marshall Space Flight Center (MSFC) are indicated in Table 2. The equipment and procedure described in this report for melting the zinc specimens apply only to the ground tests conducted at ORNL. However, all of the ground-tested capsules with the exception of B-14 were analyzed at ORNL. A complete listing of all the ground tests, test conditions, and analysis data is found in Tables 3 and 4. Table 3 lists the data for constant temperature melting tests, while Table 4 shows similar data for the gradient temperature tests.

Apparatus

Constant Temperature Furnace

A horizontal Marshall high-temperature tubular furnace was used to melt the zinc specimens at a constant temperature. The furnace was capable of producing a specimen temperature of 1315°C; a temperature controller of the on-off type was employed. An alumina boat was used to support an 11-in.-long × 2-in.-OD × 5/8-in.-ID bronze temperature leveling bar in the center of the tube furance. The zinc capsule was placed in the heavy bronze bar and sealed with two brass end plugs. The bronze bar served to reduce the temperature gradient across the zinc specimen to less than 3°C. Specimen temperature was monitored with a Chromel-Alumel thermocouple spot-welded to the center of the tantalum capsule and two similar thermocouples welded at points 1-1/4 in. to each side of the center thermocouple. A Brown recorder was used to record temperatures measured by the center thermocouple, while a Rubicon potentiometer was used to determine temperatures from the two outer thermocouples.

Two specimens (A-14 and A-15) were subjected to relatively rapid melting tests in the vertical clam-shell furnace shown in Fig. 5. The capsule was inserted in a closed copper tube (to minimize the temperature gradient) which was suspended by wire into the center of the furnace. Temperature variations across the tantalum capsule were from 5 to 20°C as measured by thermocouples spot-welded to the capsule. As before, three Chromel-Alumel thermocouples were used to measure specimen temperature. Considerably faster cool down was afforded by this furnace by opening the clam shell after the zinc had solidified.

Gradient Furnace

The gradient furnace used for M-558 ground tests at ORNL was built from drawings supplied by the Westinghouse Astronuclear Laboratory. The unit was operated in a 4-in.-diam oil-diffusion pumped vacuum system as shown in Fig. 6. However, only a 15-cfm roughing pump was used to evacuate the system to the operating pressure of $\sim 10^{-2}$ Torr. The furnace was used in a vertical position and was powered by a 120-V, 5-A Variac. The gradient furnace incorporated four Chromel-Alumel thermocouples at various locations

TABLE 3. Ground Test Data - Constant Temperature Melting Experiments for Skylab M-558

Capsule No.	Date Melted	Facility Where Melted	Soak Temp. (°C)	Soak Time	Capsule Orientation	Zn Cylinder Orientation	Section No.	Section Location	Section Weight (g)	Activity of Section (μCi/g)	Date Activity Measured	Autoradiograph Results	Remarks
B7	10-20-72	ORNL	550	16 hr	Horizontal		A B C D		0.1235 0.1502 0.1344 0.1414	1.538 1.532 0.819 0.820	10-24-72	Specimen had uniform ^{65}Zn distribution	Zn cylinder broke at bond B-C some-time during the melt.
B8	10-23-72	ORNL	550	16 hr	Horizontal		A B C D E		0.2507 0.1868 0.1485 0.2782 0.2020	1.237 1.285 1.279 1.258 1.287	10-25-72	Specimen had uniform ^{65}Zn distribution	
A11	11-2-72	ORNL	550	2 hr	Horizontal		A11-1 A11-2 A11-3 A11-4		0.1807 0.2010 0.1470 0.0593	1.595 1.595 1.580 1.650	11-8-72	Specimen had uniform ^{65}Zn distribution	A11-4 was sample drilled out from the center portion of the cylinder.
A12	11-9-72	ORNL	550	1/4 hr	Horizontal		A11-8 A11-9 A11-10	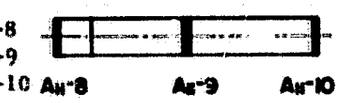	0.1302 0.2662 0.1588	1.295 1.310 1.318	11-14-72	Radiograph not taken	
A14	12-11-72	ORNL	550	~1 min	Vertical		A14-1 thru A14-48		See Appendix B-4	See Appendix B-4	12-14-72	Radiograph not taken	^{65}Zn gradient across the cylinder--both longitudinally and radially
A15	1-12-73	ORNL	550	~2 min	Vertical		N-1 thru N-60		See Appendix B-5	See Appendix B-5	1-18-73	Radiograph not taken	^{65}Zn gradient across the cylinder--both longitudinally and radially

TABLE 4. Ground Test Data - Gradient Temperature Melting Experiments for Skylab M-558

Capsule No.	Date Melted	Facility Where Melted	Capsule Orientation	Zn Cylinder Orientation	Temp. Gradient	Soak Time	Section Wt. and Activity	Date Activity Measured	Remarks
A2	11-10-72	MSFC	Vert.	^{65}Zn at bottom (cold end)	See Westinghouse data for 775°C soak temperature	2 hr	See Appendix B-1	12-7-72	Uniform ^{65}Zn distribution
A3	11-10-72	MSFC	Vert.	^{65}Zn at top (hot end)	See Westinghouse data for 775°C soak temperature	2 hr	See Appendix B-2	12-5-72	Uniform ^{65}Zn distribution
A13	11-27-72	ORNL	Vert.	^{65}Zn at bottom (cold end)	425°C-795°C	~10 min	See Appendix B-3	12-13-72	Uniform ^{65}Zn distribution
A0	12-5-72	MSFC	Vert.	^{65}Zn at bottom (cold end)	See Westinghouse data for 775°C soak temperature	1 hr	See Appendix B-6	1-23-73	Incomplete melting
A1	12-5-72	MSFC	Vert	^{65}Zn at top (hot end)	See Westinghouse data for 775°C soak temperature	1 hr	See Appendix B-7	1-22-73	Uniform ^{65}Zn distribution
B13	12-5-72	MSFC	Vert.	^{65}Zn in middle	See Westinghouse data for 775°C soak temperature	1 hr	See Appendix B-8	1-22-73	Uniform ^{65}Zn distribution

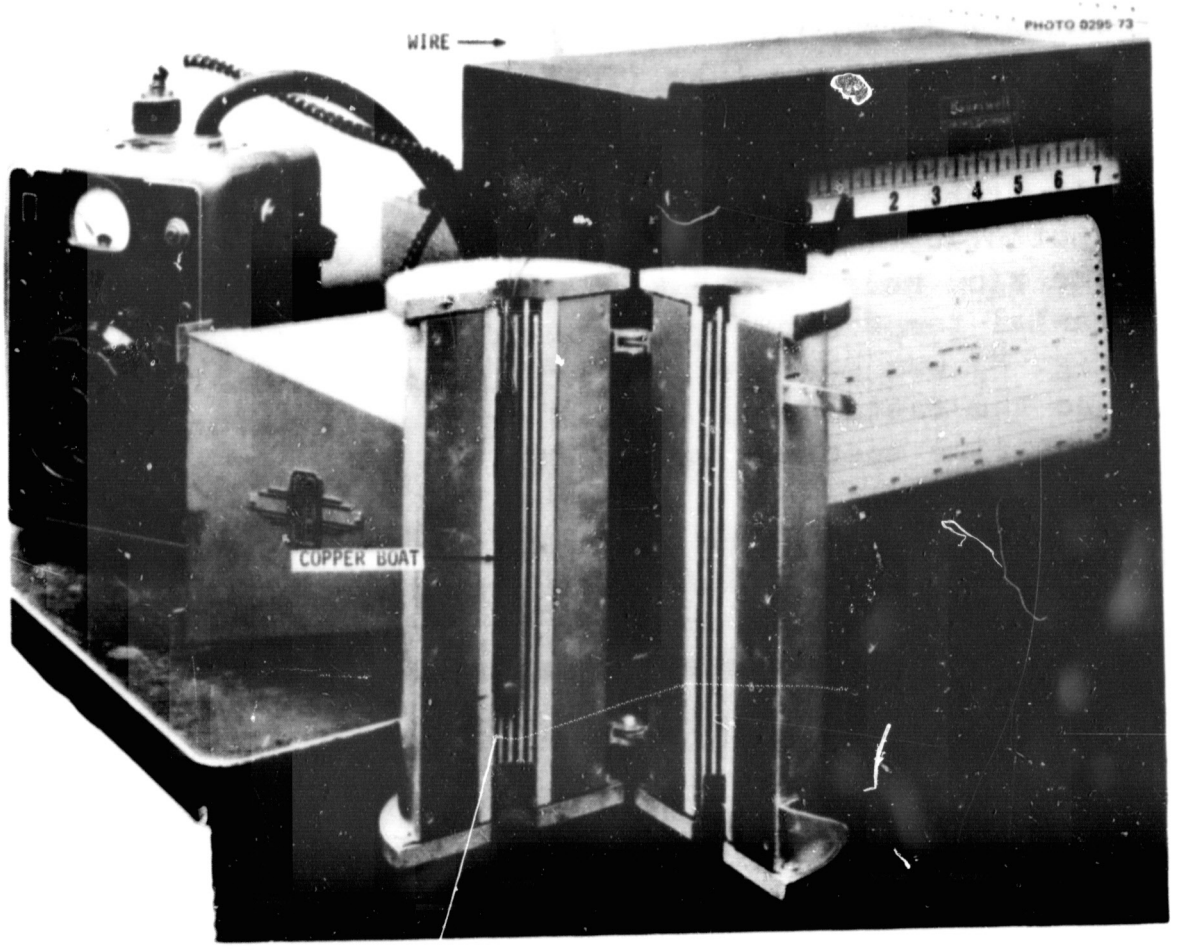

Fig. 6. Vertical Gradient Furnace in Vacuum System.

within the furnace to monitor furnace temperature. The thermocouple at the cold end of the furnace tube (TC-8) was selected as the control thermocouple and was calibrated against the temperature determined for the cold end of a zinc dummy specimen as measured by a thermocouple spot-welded to the tantalum tube. Figure 7 is a graph of that calibration made using the Rubicon potentiometer. For the "cold" end of the zinc specimen to be just above the zinc melting point, 420°C, the control thermocouple read 290°C. The axial temperature gradient across the zinc specimen at this point (see Fig. 8) was measured by three Chromel-Alumel thermocouples spot-welded to the tantalum capsule as previously described. When the cold end of the zinc specimen was 420°C, the hot end was 790°C.

Tantalum capsules tested in the vertical gradient furnaces were first enclosed in a thin-walled stainless steel cartridge under argon as shown in Fig. 9. The capsule was held in place by two carbon inserts and was insulated across its center by Fiberfrax material. Disks of quartz cloth served

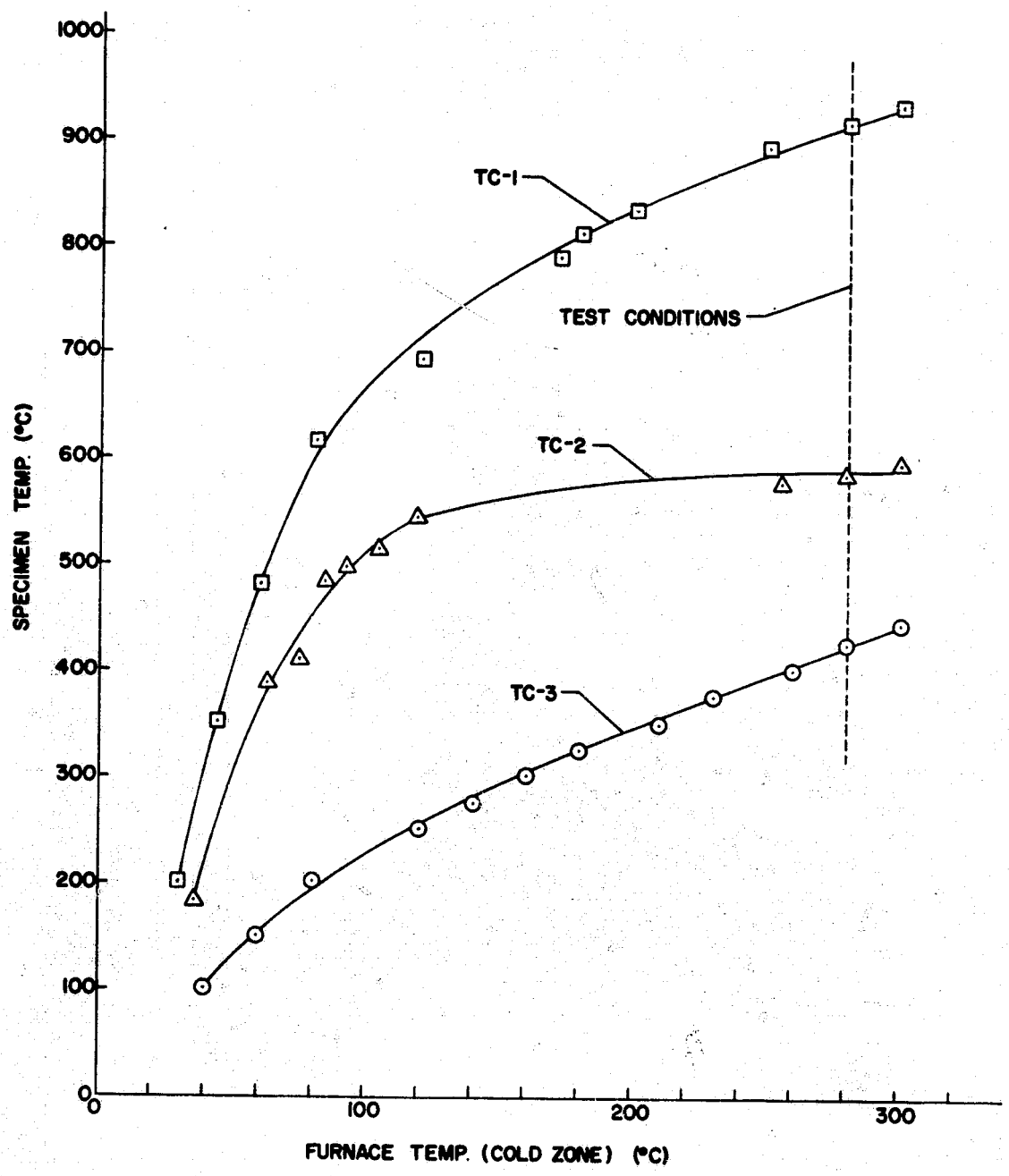

Fig. 7. Calibration of Vertical Gradient Furnace.

as spacers. A copper tube at one end was used to evacuate and backfill the cartridge with helium; this tube was sealed by crimping. The cartridge was subsequently mounted in the furnace and subjected to temperatures that produced the temperature gradient across the zinc specimen as shown in Fig. 8. It should be pointed out that all calibrations and melting tests conducted with the vertical gradient furnace were made using the stainless steel cartridge to simulate as closely as possible the actual flight experiment.

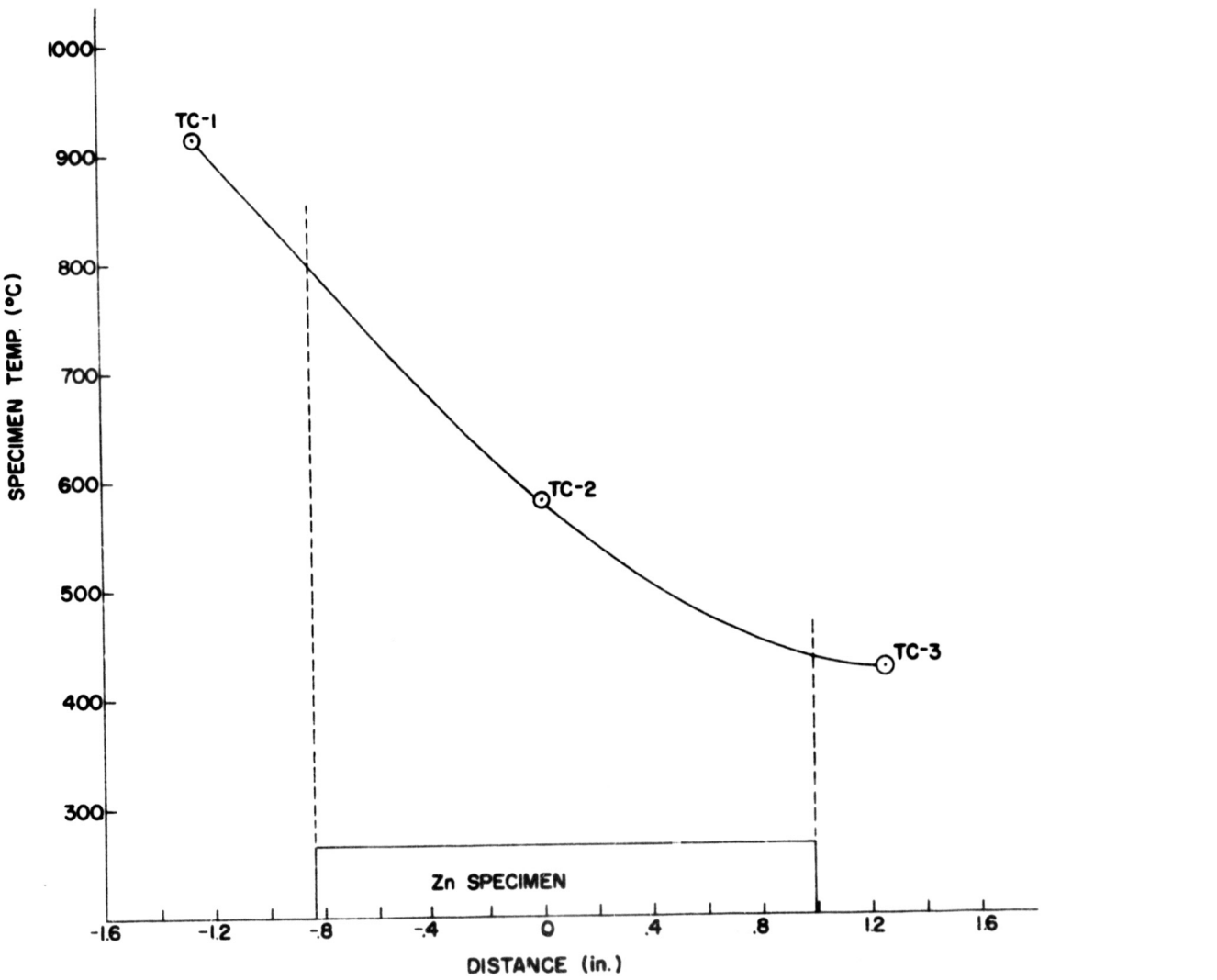

Fig. 8. Temperature Distribution Across Zinc Specimen in Vertical Gradient Furnace.

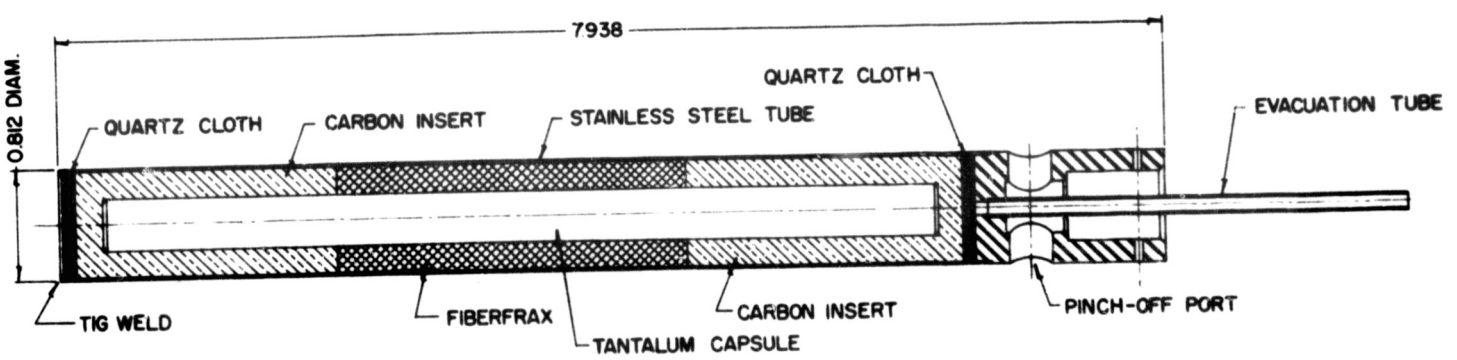

Fig. 9. Stainless Steel Cartridge Containing a Tantalum Capsule — Used for Melting Tests in Gradient Furnace.

Specimen Analysis

Autoradiography

Several of the zinc specimens (B-7, B-8, A-11) were cut in half longitudinally and autoradiographed before sectioning. This was accomplished by laying the half-specimen, flat side down, on Kodak NTB film for 16 hr and then developing the film. This analysis scheme was dispensed with in favor of the more accurate and quantitative machine-sectioning of zinc specimens as full round bars rather than half sections followed by counting of radiation intensity.

Rough Sections

On many of the tested specimens, several 0.030-in. to 0.040-in. long sections were cut from different portions of a specimen using a 0.030-in.-thick diamond cut-off wheel. The activities of these sections were subsequently counted in 4 π geometry to determine the general ^{65}Zn distribution after a respective melting test. This analysis procedure was used as a quick check of the ^{65}Zn distribution across the specimen before precision machining was performed.

Precise Sectioning

Precise sectioning of furnace-melted zinc bar specimens was achieved by machining off approximately 0.040-in. transverse sections along the cylindrical axis with an Edelstaal Unimat jeweler's lathe (see Fig. 10). The metallic shavings from each cut were collected in a small aluminum pan fixed beneath the chuck of the lathe and adjacent to the tool post. These shavings were loaded through a plastic funnel into pre-weighed plastic envelopes. The plastic envelopes were then heat sealed and reweighed on a Mettler microbalance to determine the zinc section weight (by difference). As the requirements for additional analysis developed, it was decided to perform radial sampling at every sixth or seventh section. This involved machining and dividing a section into two or three approximately equal parts (by weight) between the outer surface and the center of the cylindrical bar. In this way, it was possible to analyze the radial distribution of ^{65}Zn in the specimen as well as the longitudinal distribution.

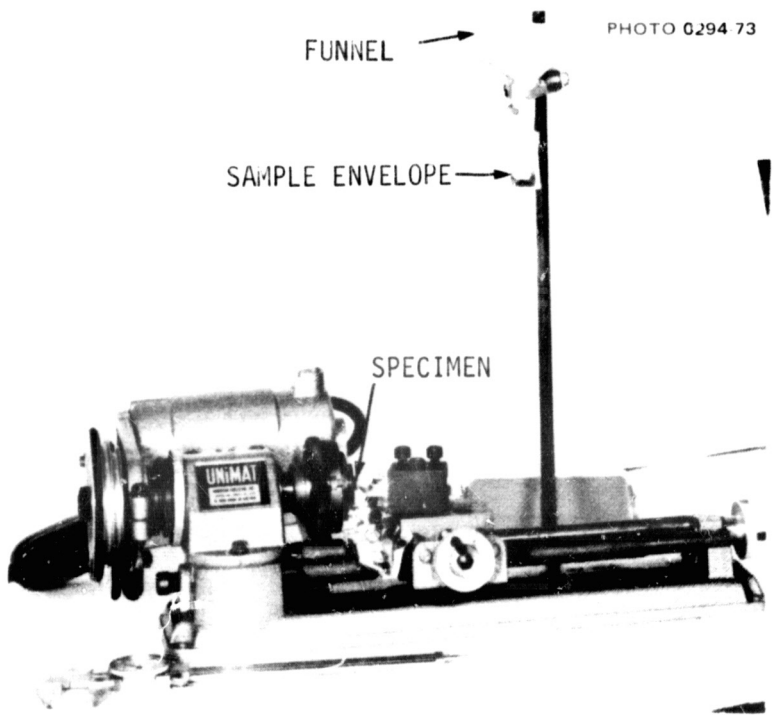

Fig. 10. Jeweler's Lathe Used for Precise Sectioning of Zinc Specimens.

Gamma Counting

The zinc specimens were counted, after melting and before sectioning, in a gross ionization chamber at ORNL to determine the total ^{65}Zn activity. The activities of the zinc sections or shavings were measured using a low-level gamma-ray spectrometer. This latter system uses two opposed 5- by 4-in. NaI detectors in a cabinet shielded with 5-in.-thick lead walls. A 256-channel multichannel analyzer was used for data acquisition. In the mode of operation used, the gain of the two detectors was matched and their outputs were summed, thus giving the capability of measuring picocurie amounts of gamma radioactivity.

Results

Constant Temperature Tests

Zinc specimens were heated to 550°C in the horizontal Marshall furnace and allowed to soak for time periods of 16, 2, and 1/4 hr as listed in Table 3. Rough sectioning and counting, as well as autoradiographs, proved that ^{65}Zn was uniformly distributed throughout the specimens (see B-7, B-8, A-11, and A-12, Table 3).

Specimens A-14 and A-15 were heated in the vertical clam-shell furnace according to the temperature—time history shown in Fig. 11. Sample A-14 was held above the melting point for about 6 min with a peak temperature of 550°C, while sample A-15 was held for about 10 min at the same peak temperature. Note that the effect of the heat of fusion during melting

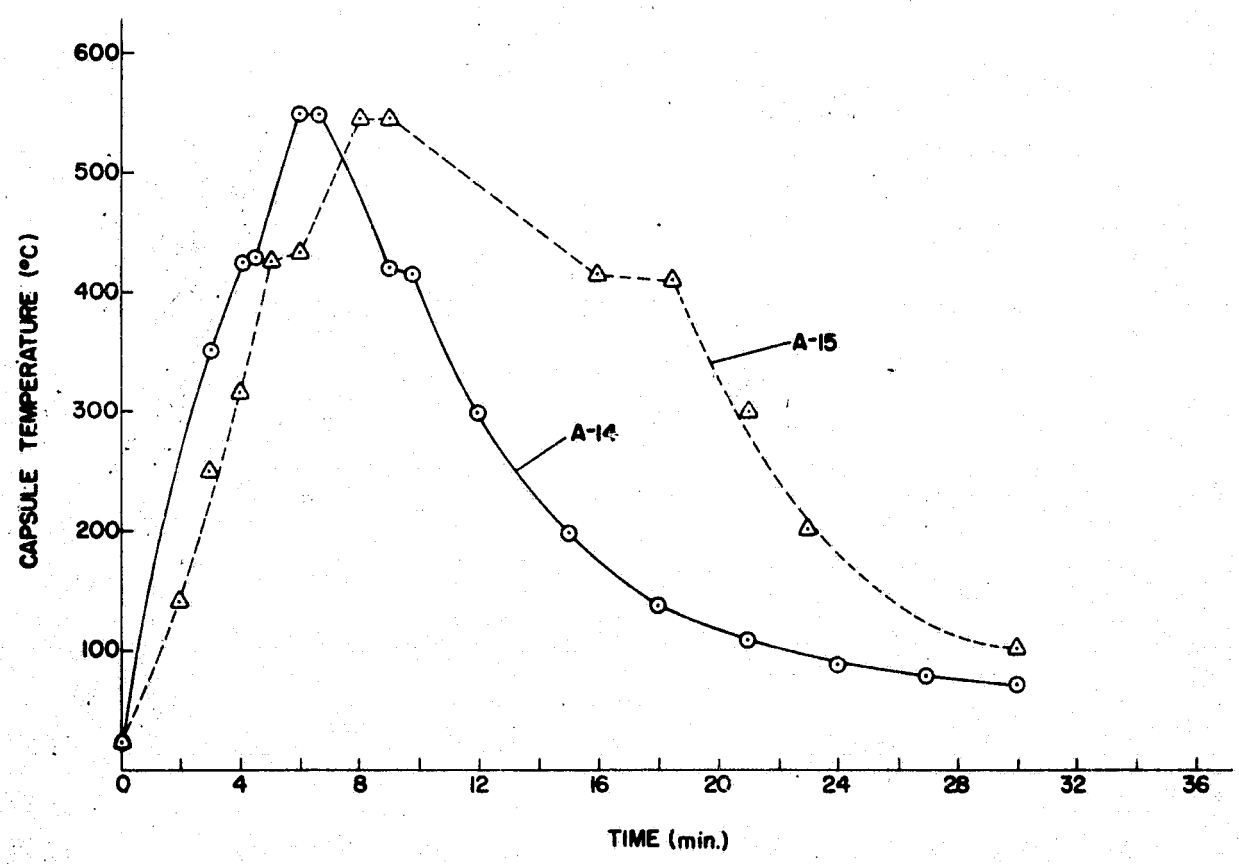

Fig. 11. Time—Temperature History for Capsules A-14 and A-15.

and freezing of the zinc is easily observed on the thermal recorder traces for both runs. The distribution of ^{65}Zn across sample A-14 is shown in Fig. 12. (The data used in this plot are listed in Appendix B.) A ^{65}Zn concentration gradient was produced by the melting test which appeared to decrease from the ^{65}Zn-labeled end in steps. Data on the radial distribution in three sections are shown by the squares and diamonds. These radial data clearly indicate that in this rapid melting test, the ^{65}Zn moved more rapidly through the center of the cylindrical bar than through the outer sheath of material. Since the average level of radioactivity in the radial sections lies on the gradient line (triangular data points), it is presumed that most of the other section activity levels are also averages of this nonuniform distribution.

The longitudinal ^{65}Zn distribution for sample A-15 is shown in Fig. 13. The ^{65}Zn concentration gradient was less steep, in this case, than the one demonstrated by sample A-14 in Fig. 12, but still retained the steps, or waves, in the curve. That data shown as triangles in this figure

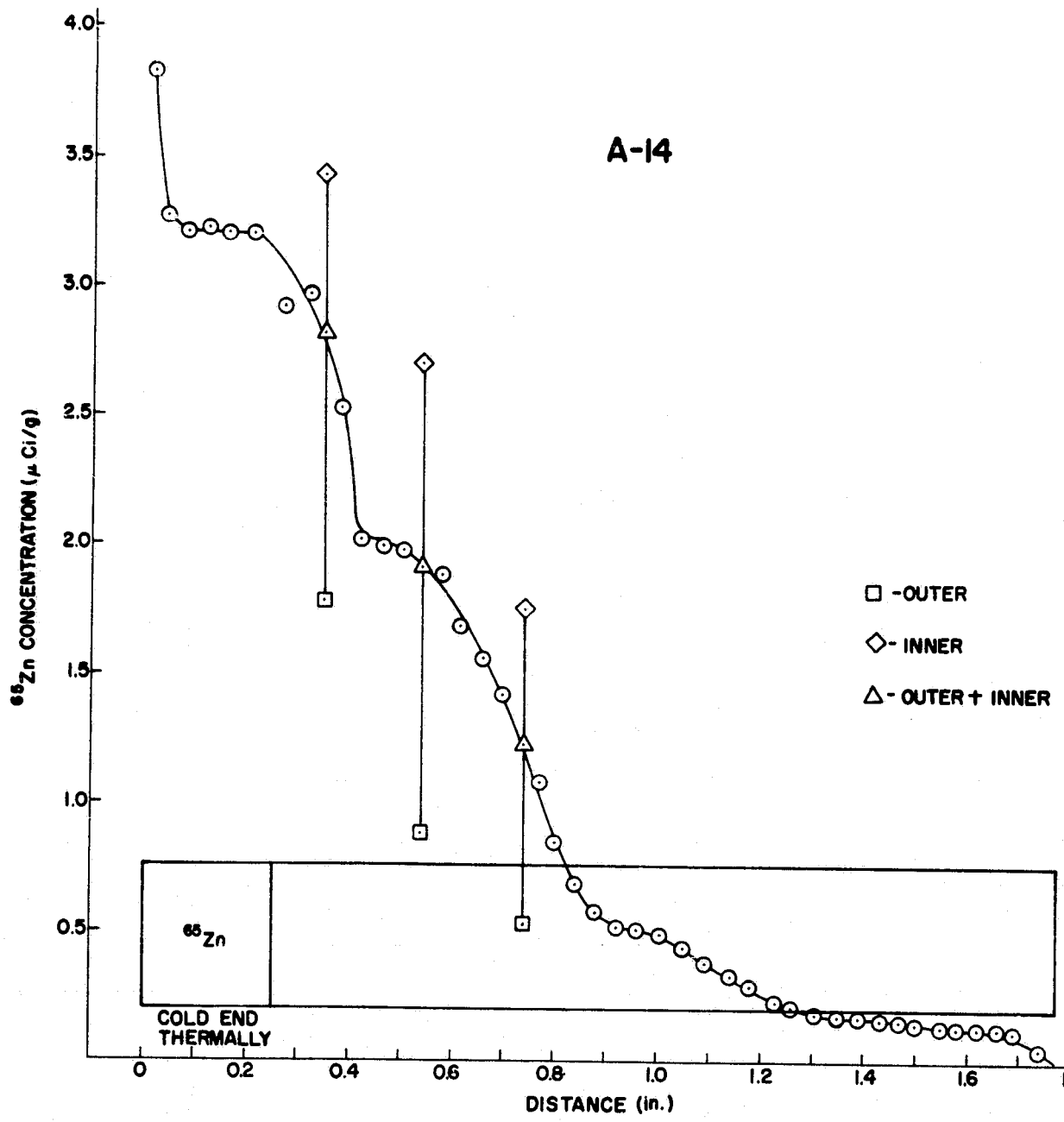

Fig. 12. Zinc-65 Concentration Gradient in Specimen A-14 After Melting.

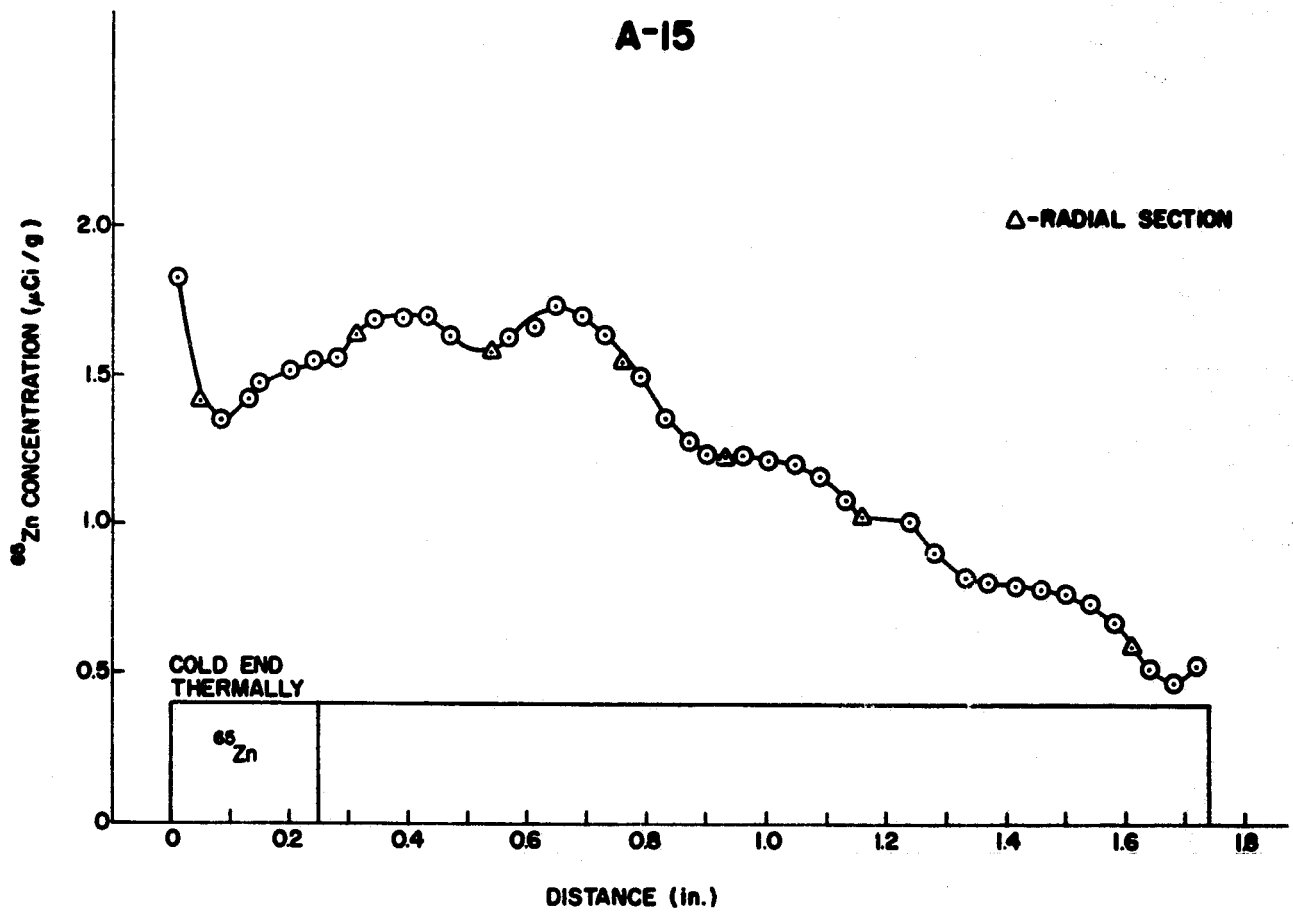

Fig. 13. Zinc-65 Concentration Gradient in Specimen A-15 After Melting.

represent the average ^{65}Zn concentration in three radial sections analyzed at those points along the specimen. A separate plot of these values shows the radial distribution of ^{65}Zn in sample A-15 at these points (see Fig. 14). Several obvious qualitative results can be derived immediately from the figure, but quantitative assessment is left to the principal investigator. First one can observe that, as before, the ^{65}Zn moved more rapidly through the sample center than along its periphery. This produced ^{65}Zn-rich centers at the top of the specimen and ^{65}Zn-lean centers at the bottom. Note also that the profile nearest the bottom and through the original ^{65}Zn pellet contained less ^{65}Zn than the section just above the ^{65}Zn–Zn interface.

Gradient Temperature Tests

The results of melting tests on capsules A-2, A-3, A-13, A-0, A-1, and B-13 in the Westinghouse gradient furnace (in the vertical position) are listed in Table 4. All of the capsules except A-13 were melted at MSFC. The temperature–time history for these capsules is shown in Fig. 15. The specimen temperature on the ordinate is normalized to permit comparison of data from ORNL and MSFC where different control thermocouples were used. It is seen that capsules A-2 and A-3 were held for longer times above the melting point than were capsules A-0, A-1, and B-13 and that capsule A-13 was held above 420°C for a shorter time than any of the others. Note also that these time periods are much longer than those recorded for capsules A-14 and A-15 that were melted in the vertical clam-shell furnace at ORNL.

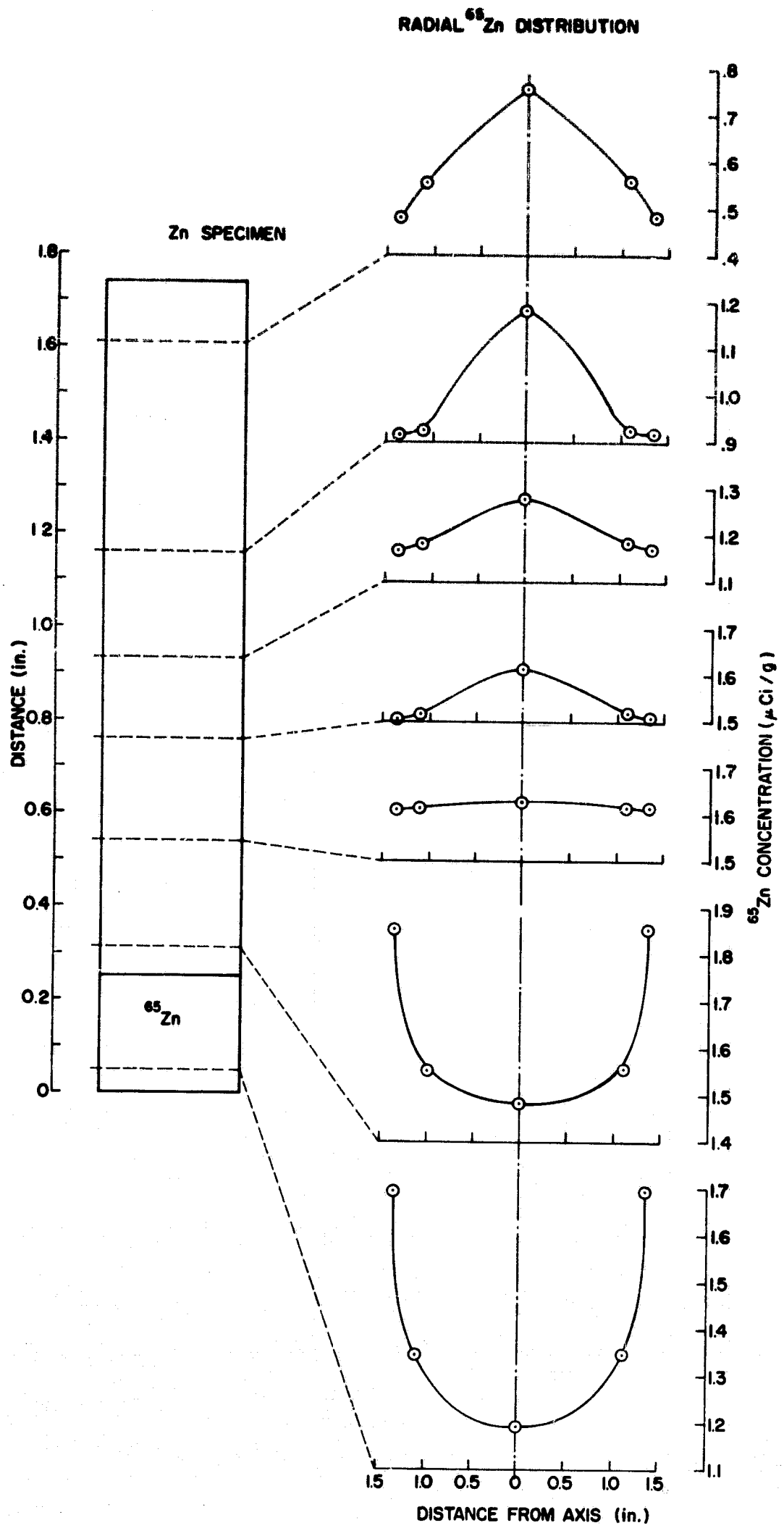

Fig. 14. Radial ^{65}Zn Distribution in Specimen A-15 After Melting.

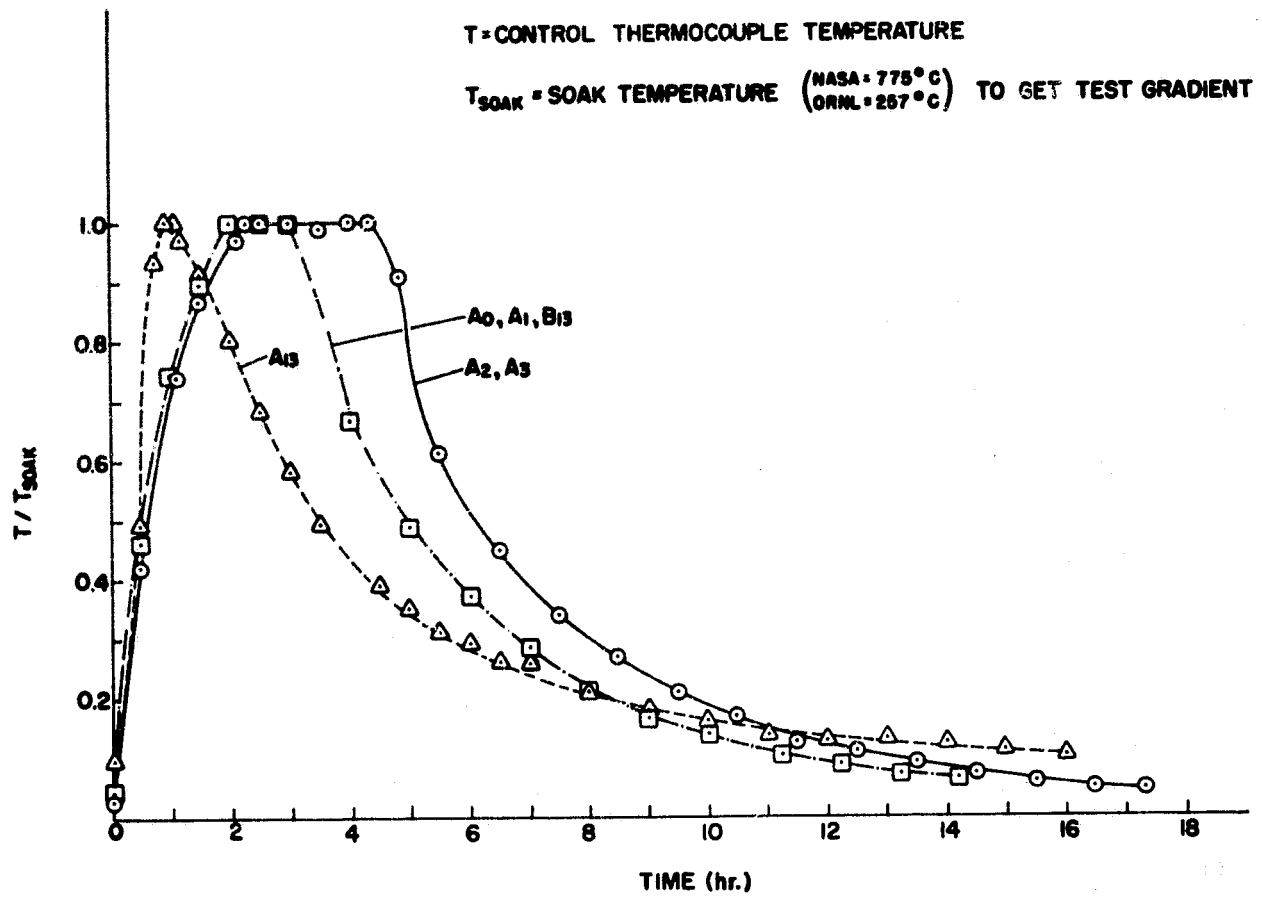

Fig. 15. Time—Temperature History for Capsules A-13, A-2, A-3, A-0, A-1, and B-13.

The ^{65}Zn distribution after melting is shown for samples A-2, A-3, A-13, A-0, A-1, and B-13 in Figs. 16 through 21, respectively. The figures show that all of the zinc specimens tested in the gradient furnaces had a uniform distribution of ^{65}Zn in the longitudinal direction. Radial sections were also analyzed which consisted of an outer half (by weight) and an inner half which are shown by the diamond and square data points, respectively. The data for these sections (see Appendix B) show that the specimens were also uniform in the radial direction. Whether the ^{65}Zn pellet was located at the thermally cold end (A-2, A-13, A-0) or at the thermally hot end of the furnace (A-3, A-1) made no difference in the final distribution for the times and temperature gradients used. However, one anomaly in the results is seen for specimen A-0 in Fig. 19. Three sections of very high ^{65}Zn concentration were found at the thermally cold end of the specimen. Since the activity contained in these sections approached that of the original ^{65}Zn pellet, it was assumed that these sections were not melted during the test.

It seems quite clear from these results that zinc transport in molten zinc is so rapid that it would be virtually impossible to create a ^{65}Zn concentration gradient using existing flight hardware in a unit-gravity environment. The results for samples A-14 and A-15 indicated that only 15 or 20 min at temperatures above the melting point of zinc were sufficient to produce a completely uniform ^{65}Zn distribution. These results demonstrated that in addition to diffusion, convectional forces were strongly affecting the zinc transport process.

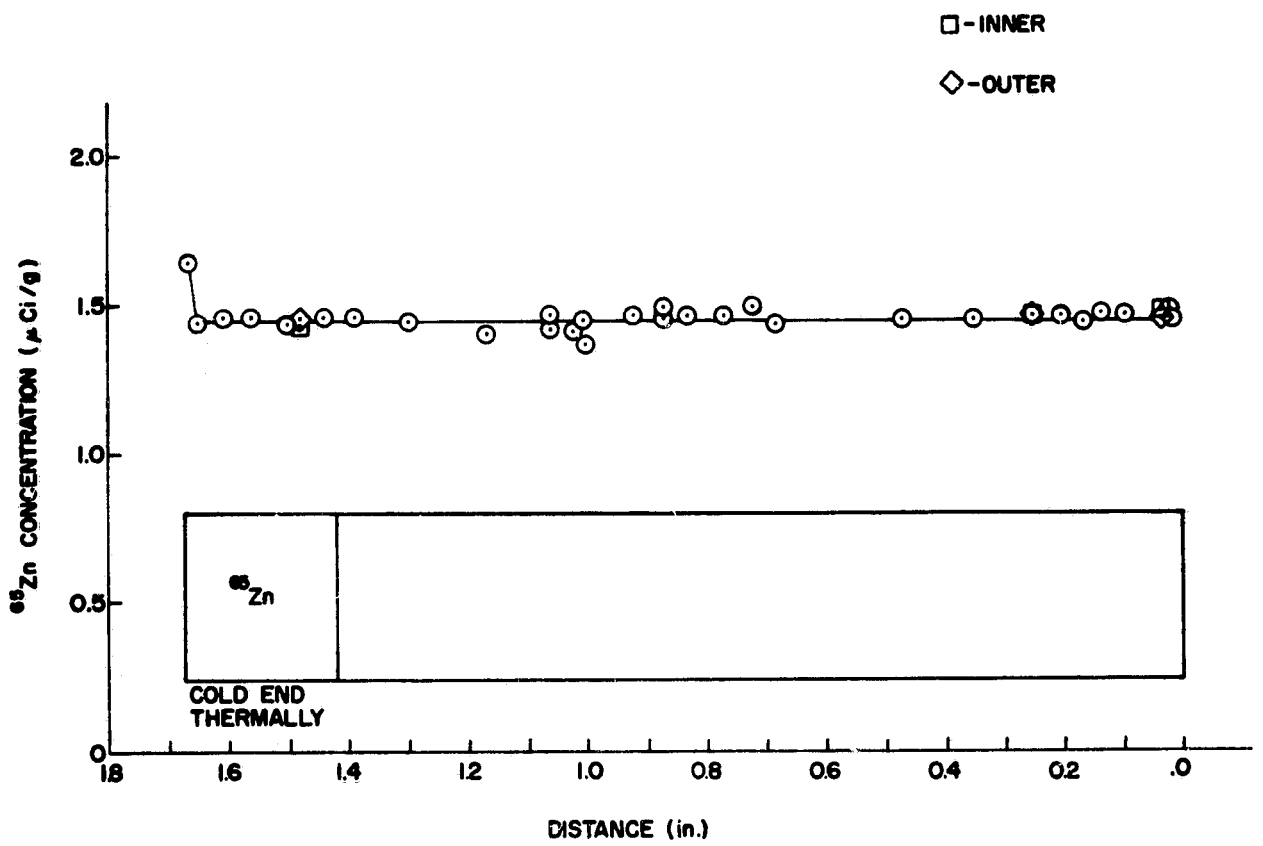

Fig. 16. Zinc-65 Concentration Gradient in Specimen A-2 After Melting.

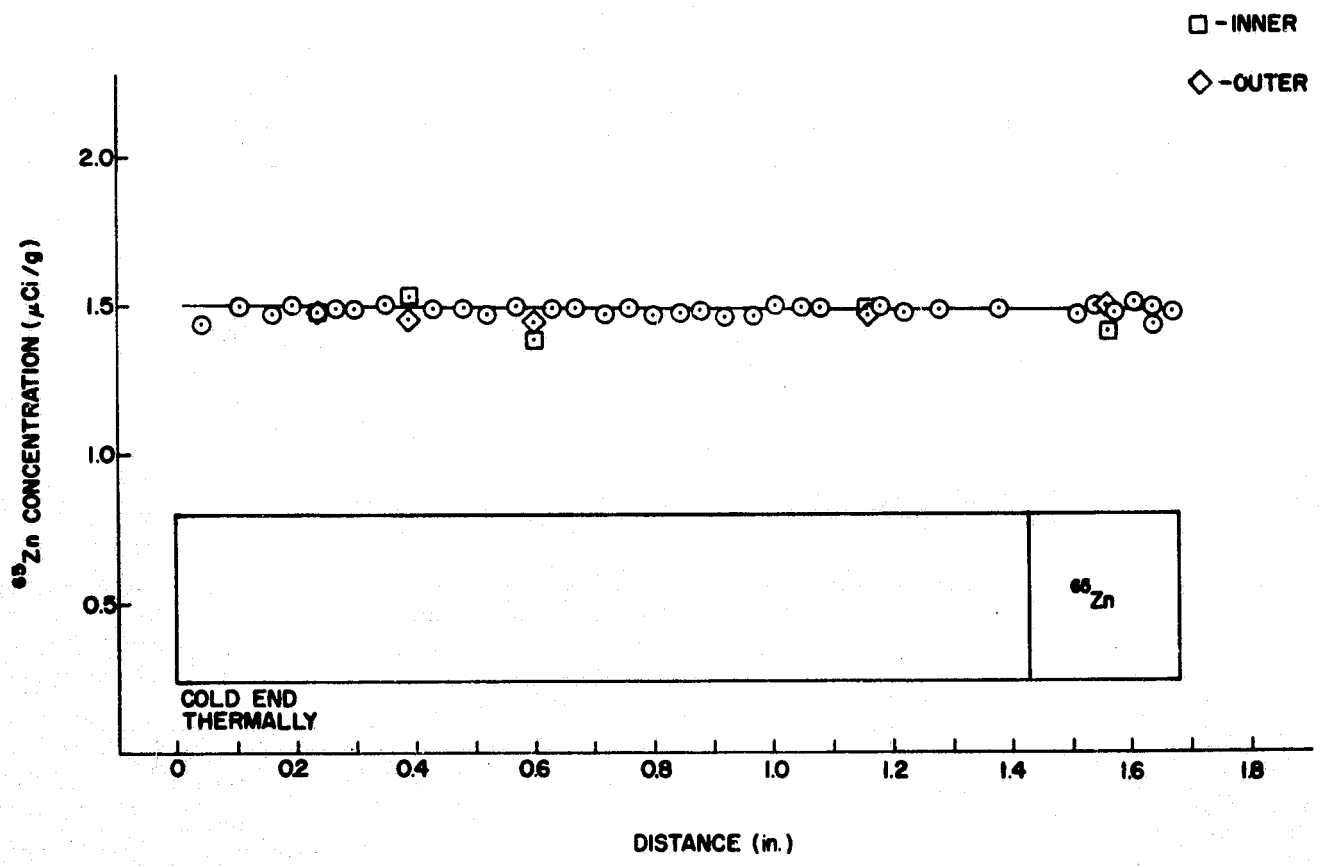

Fig. 17. Zinc-65 Concentration Gradient in Specimen A-3 After Melting.

A-13

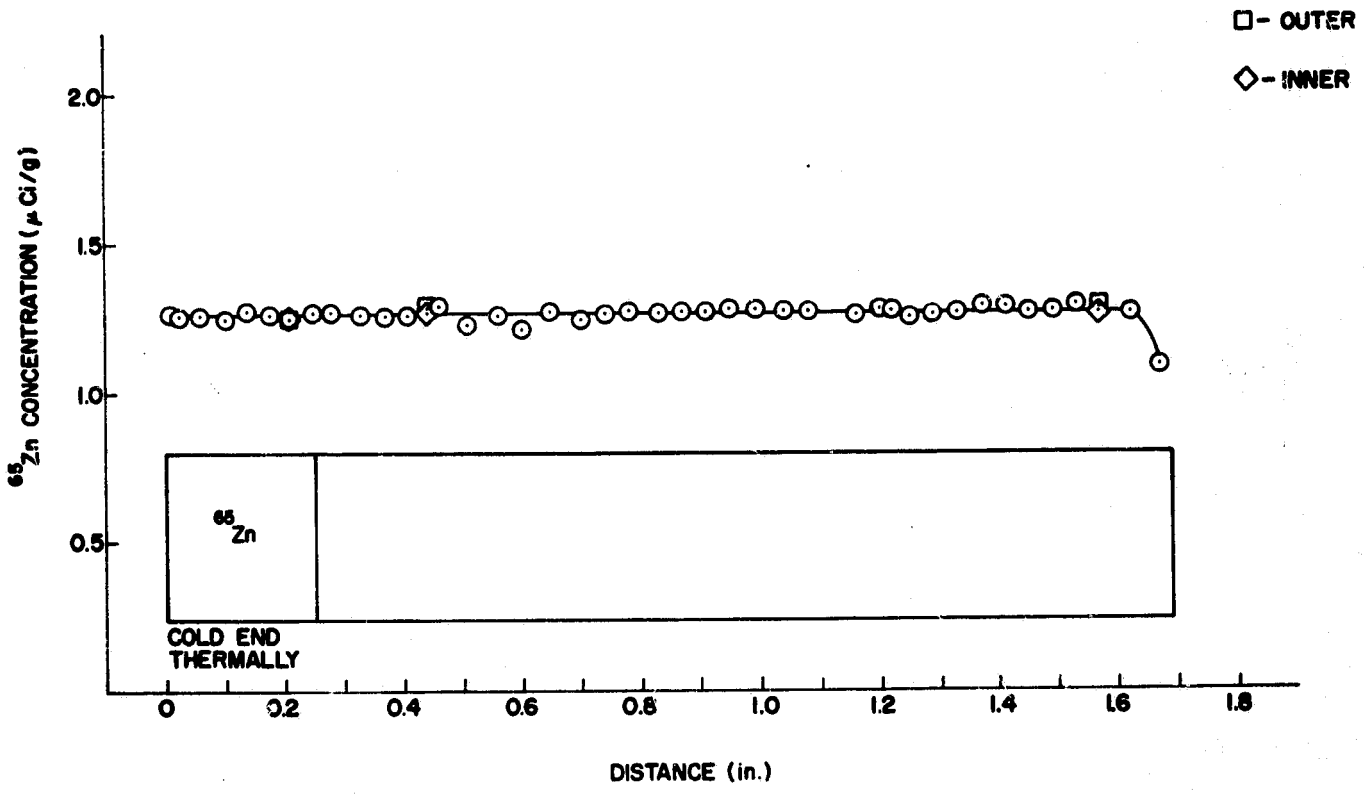

Fig. 18. Zinc-65 Concentration Gradient in Specimen A-13 After Melting.

A-0

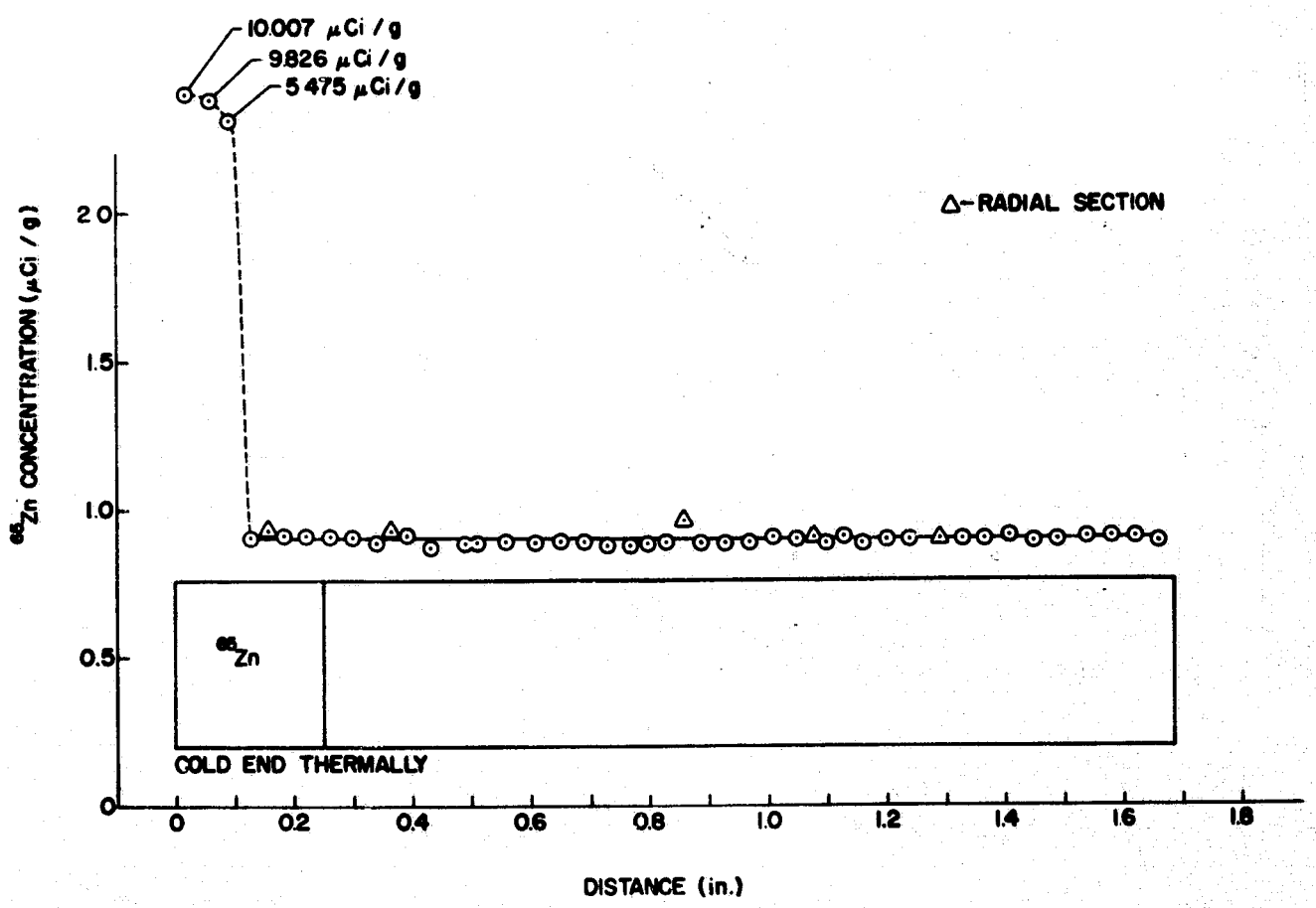

Fig. 19. Zinc-65 Concentration Gradient in Specimen A-0 After Melting.

A-1

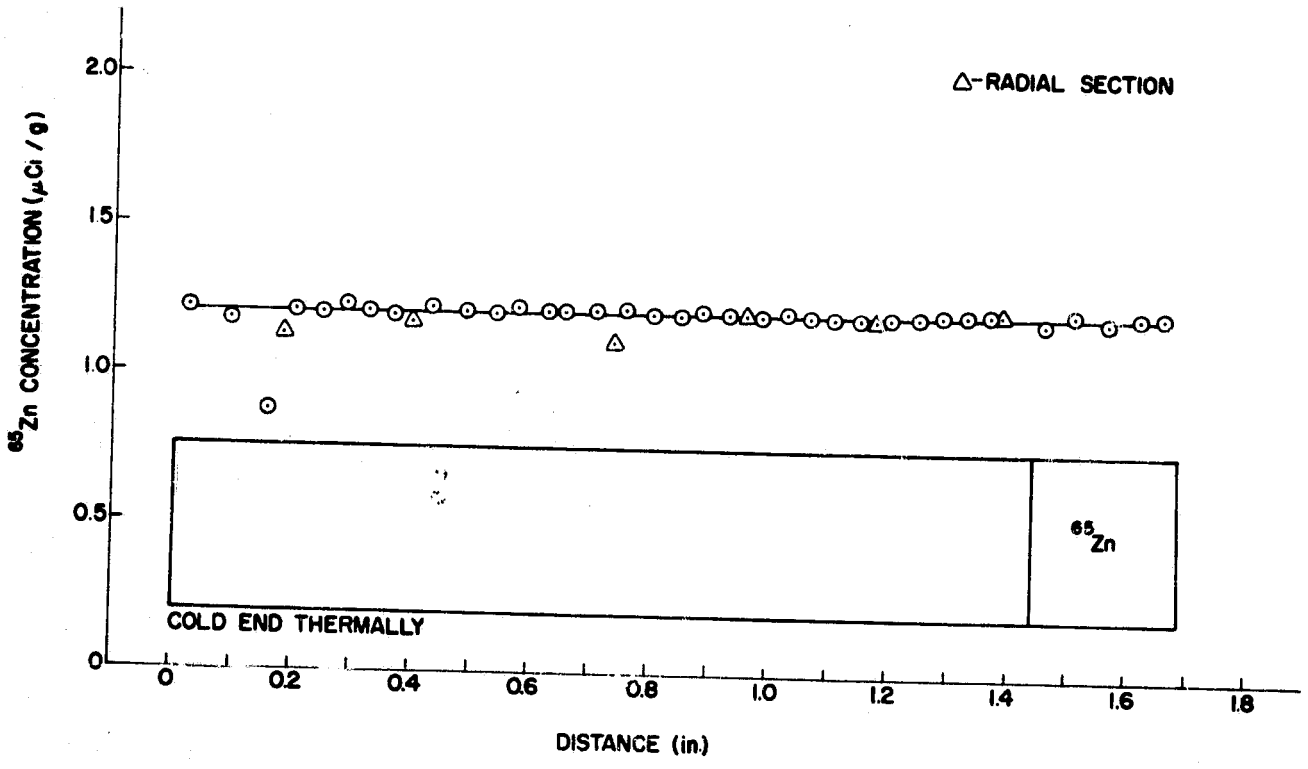

Fig. 20. Zinc-65 Concentration Gradient in Specimen A-1 After Melting.

B-13

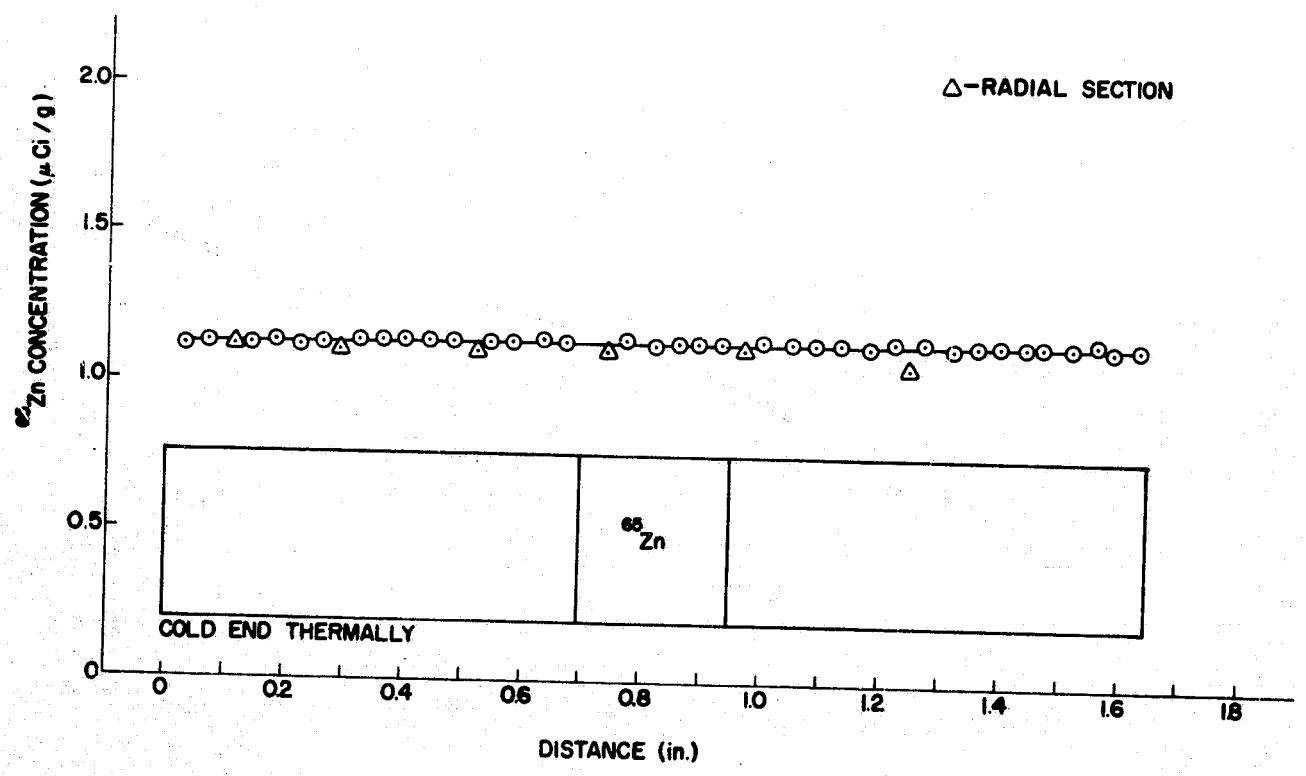

Fig. 21. Zinc-65 Concentration Gradient in Specimen B-13 After Melting.

FLIGHT SAMPLE ANALYSIS

Physical Measurements of Zinc Samples After Flight

Zinc samples A-6, A-7, and B-5 (see Table 5) were removed from the tantalum capsules by cutting the tubes near the weld closures. This was accomplished using a lathe and a small metal cutting saw. After removal, the zinc samples were photographed using a Polaroid MP-3 camera and Type 52 sheet film. The length and average diameter of each zinc sample were measured using a direct reading caliper, while the weight was determined using a Mettler M-5 microbalance. The total ^{65}Zn activity in each sample was measured in a gross ionization chamber.

Table 5. Physical Parameters of Zinc Samples Used in Flight Experiments

Capsule No.	Sample Weight (g) Before Melting	Sample Weight (g) After Melting	Sample Length (in.) After Melting	Sample Diameter (in.) After Melting	Sample Activity (μCi) After Melting	Date Activity Measured
A-6	13.5846	13.5807	1.876	0.291	8.34	10-16-73
A-7	13.6367	13.6349	1.892	0.287	7.75	10-16-73
B-5	13.5613	13.3650	1.829	0.290	7.32	10-16-73

Precise Sectioning

To determine the axial ^{65}Zn distribution in the three Skylab samples A-6, A-7, and B-5 after melting in space, each was machined into approximately 0.040-in.-thick transverse sections (see p. 16) which were accurately indexed. An Edelstaal Unimat jeweler's lathe with an ultrasharp tool bit was used to cut the transverse sections into shavings which were quantitatively collected and heat sealed in preweighed plastic envelopes. Each envelope containing the zinc shavings was subsequently reweighed to determine the zinc section weight (by difference). Every sixth or seventh section was machined and packaged in a manner to permit analysis of the ^{65}Zn concentration as a function of radial distance. This was accomplished by machining a transverse section into three approximately equal parts (by weight) accurately indexed between the outer surface and the axis of the zinc sample. The first radial portion of the section to be machined off was designated an "outer" (O) radial section, followed by "middle" (M) and "inner" (I) radial sections. The combined activity of the three O-M-I sections was equivalent to a whole section and could be plotted as such.

Gamma Counting

The gamma intensity from each envelope of zinc shavings was measured using a low-level gamma-ray spectrometer, the same instrument as was employed for the ground-test samples. (This system utilizes two opposed 5- by 4-in. NaI detectors, which, for small samples, provides essentially a

4 π geometry.) Once the ^{65}Zn radiation intensity for a particular sample section was determined (in microcuries), it needed only to be divided by the weight of that section (in grams) to produce a value of the relative ^{65}Zn concentration. Values of ^{65}Zn concentration were finally plotted as a function of location in the original zinc sample.

Results of Physical Measurements

Photographs of the Skylab M-558 samples A-6, A-7, and B-5, obtained immediately after removal from their tantalum capsules, are shown in Fig. 22. Figure 22a shows the zinc samples with their central axes parallel to the page; Fig. 22b is a similar view, but the samples have been rotated 180° to expose the opposite side to that seen in Fig. 22a. Figure 22c is an end view of the samples with the ^{65}Zn ends of samples A-6 and A-7 facing the camera, while the opposite ends are viewed in Fig. 22d. One can immediately observe from these photographs that the bond lines or interfaces between the ^{65}Zn pellets and the unactivated zinc samples remained visible after melting in space. This result is similar to that observed for samples melted on earth. However, the wrinkled surfaces of the Skylab samples are unique and were not observed on the ground-test samples. The wrinkled surface extended completely around the samples and was probably caused by solidification shrinkage and/or a surface effect occurring during cooling. Solidification shrinkage observed for ground-test zinc samples always manifested itself as a "pipe" or depression on the top surface of the sample. On Skylab, with gravity forces near zero, one might ideally expect a complete absence of shrinkage depressions or pipes. In other words, solidification shrinkage would be uniform along the sample and a uniform sample with rounded ends (due to surface tension) would be anticipated. The presence of "wrinkles" in the Skylab samples might be explained by more rapid heat removal at selective sites along the sample. During cooling, some portions of the zinc sample would touch the wall of the carbon crucible, thus possibly conducting heat away from the zinc more rapidly in those areas. This phenomenon, in turn, could set up perturbations or movements in the liquid zinc surface which would subsequently form the wrinkles. Wrinkles occurred in those portions of the zinc samples which were located in the hot end of the furnace, as shown in Fig. 22a on the left hand portion of B-5 and A-7 and on the right hand portion of A-6. The last of the zinc to solidify formed the concave ends seen in A-7 (Fig. 22c) and A-6 (Fig. 22d). This characteristic was probably caused by the outer surface of the sample being slightly cooler than the core. In contrast, the sample ends in the cold zone of the furnace were the first to solidify and were rounded similar to the shape reached in the liquid state. (See samples B-5 and A-6 in Fig. 22c and A-7 in Fig. 22d.) At the cooler end the effects of shrinkage would be minimal because of an adequate supply of liquid zinc to feed the advancing solidification zone. Although some of the observations of the zinc sample geometries can be explained, more experimentation would be needed to fully understand this phenomenon.

Results of other measurements made on the Skylab samples are given in Table 5. All of the samples, especially B-5, showed a loss in weight,

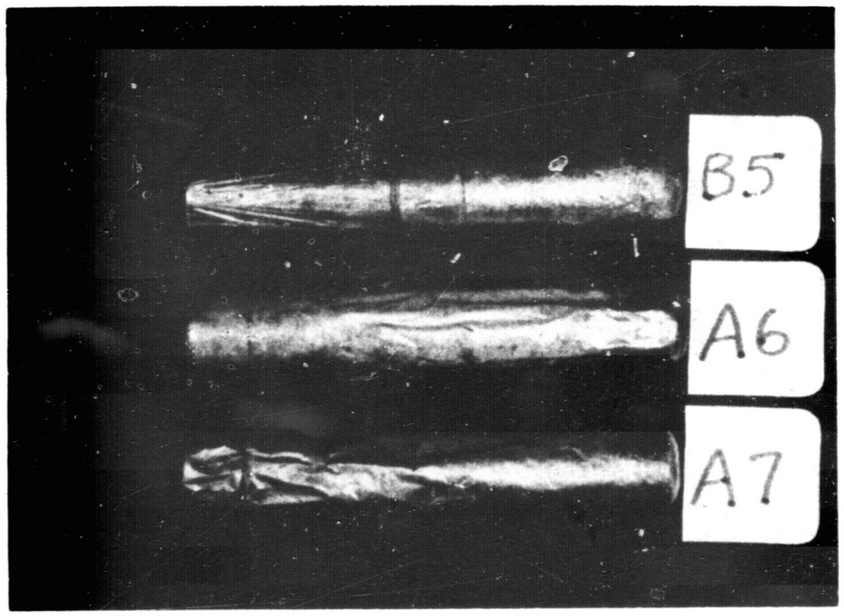

(a)

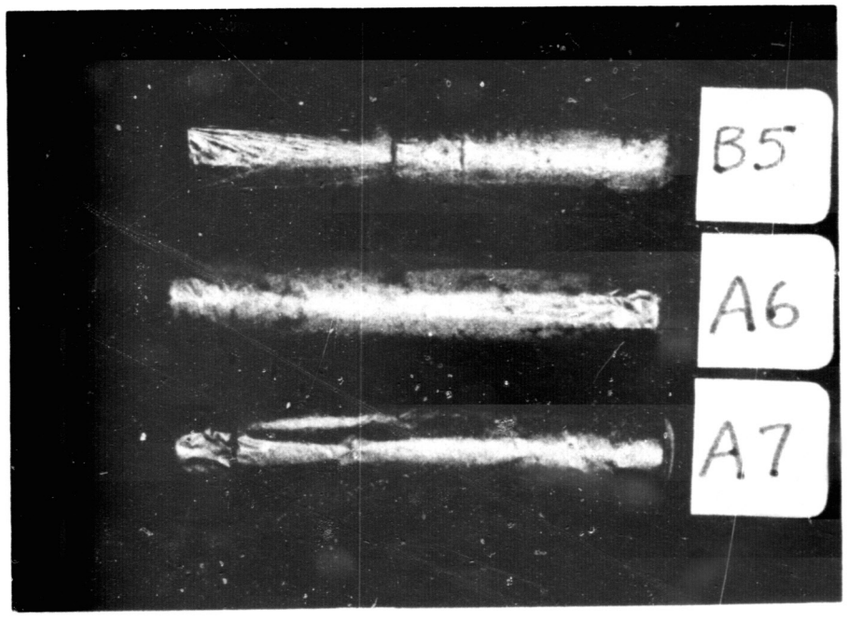

(b)

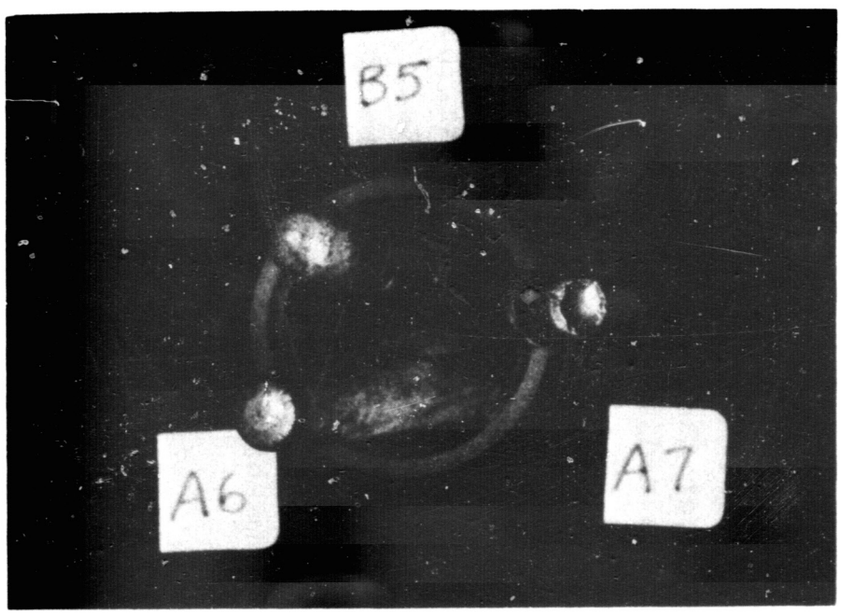

(c)

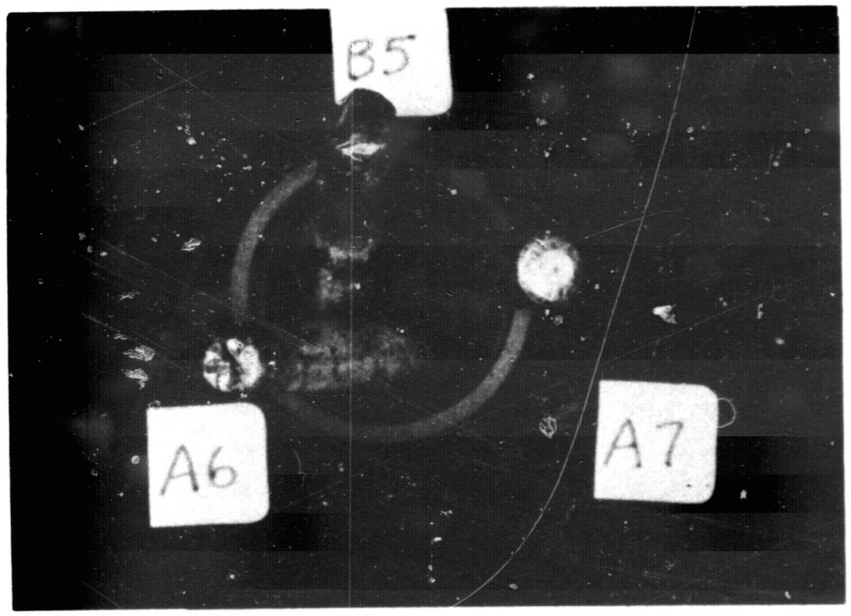

(d)

Fig. 22. Visual Observations of Skylab-III Zinc Diffusion Samples.

(a) Side View
(b) Side View — 180° Axial Rotation From (a)
(c) Sample End Views
(d) Sample End Views — Inverted From (c)

probably the result of a slight amount of zinc vaporization; this is similar to those losses observed in earth tests (p. 7). Lengths and diameters of the Skylab samples were not appreciably altered by melting in space. Obviously, values for these parameters are nominal since accurate measurements were not feasible because of wrinkled surfaces and rounded ends. Nevertheless, dimensional measurements on Skylab samples did differ from those made on similar samples melted on earth (p. 7); the sample length decreased and its diameter increased after melting and solidification in space. Changes in the physical dimensions of the earth-melted samples were almost certainly influenced by gravity.

In Table 5 radiation intensity from each sample is listed; these values may be compared with the sums of the separate intensities measured for the machined sections (see Appendices C, D, and E), thus indicating how much zinc was lost in the sectioning process for each sample. Material losses did not affect the accuracy of the analysis because the data were normalized on a concentration basis.

Distribution of ^{65}Zn in Skylab Samples

Skylab Sample A-6

The axial ^{65}Zn concentration gradient for sample A-6 is shown in Fig. 23. This sample was held at a constant temperature gradient for one hour in Skylab with the ^{65}Zn pellet located at the cold end of the gradient furnace. This heat treatment produced a sharp ^{65}Zn concentration gradient that extended to approximately the midpoint of the zinc sample. At distances >1.1 in., from the end originally containing the ^{65}Zn isotope, only the radiation intensity of every fifth section was measured because it was obvious that the ^{65}Zn concentration beyond that distance was essentially zero. The radiation intensity, weight, and location of each machined transverse section plotted in Fig. 23 are also given in Appendix C. The tabulated and graphic analytical results are markedly different than those obtained for sample A-0 which was melted for one hour in the gradient furnace on earth (see p. 23). Except for a small unmelted portion at the cold end, A-0 exhibited uniform ^{65}Zn distribution across the entire length of the zinc sample. One can immediately conclude from this comparison that the absence of gravitational forces on Skylab virtually eliminated the movement of ^{65}Zn by a convective mechanism. The smooth "textbook" ^{65}Zn concentration gradient would tend to support the theory that diffusion was the main mechanism of transport.

The radial ^{65}Zn distribution for sample A-6 is shown in Fig. 24. Radial sections taken at low ^{65}Zn concentrations near the middle of the sample demonstrate a uniform ^{65}Zn distribution. Sections within and just outside the ^{65}Zn pellet had nonuniform ^{65}Zn distributions. The sharp ^{65}Zn concentration gradients in the outer surfaces in these latter sections suggest that surface diffusion or surface tension induced convection may have influenced the movement of the ^{65}Zn. Radial distributions of ^{65}Zn for sample A-6 were slightly more uniform than those measured for the

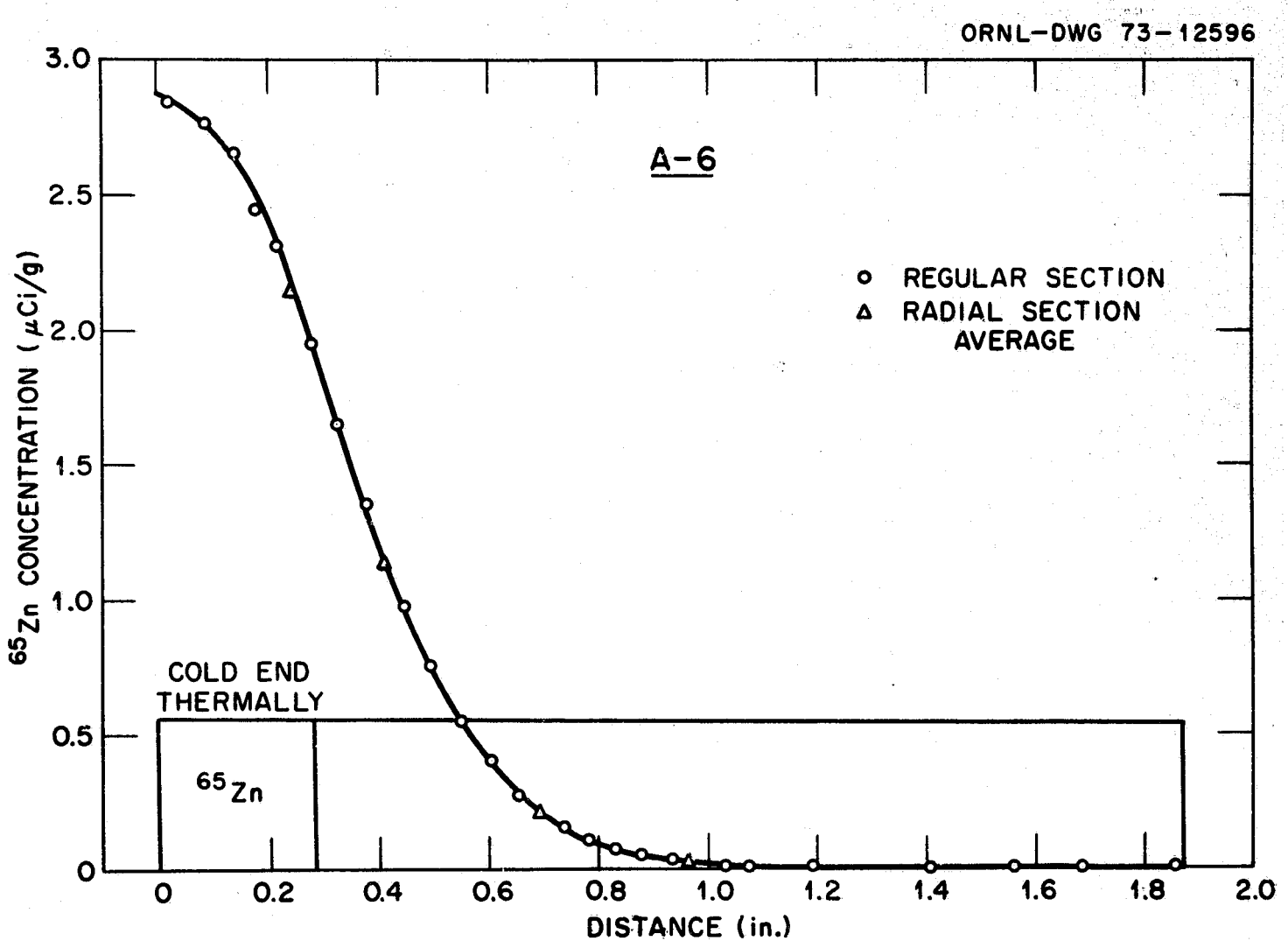

Fig. 23. Zinc-65 Axial Concentration Gradient in Sample A-6.

comparable earth sample A-0 (see pp. 23, 44, and 45) and far more uniform than those for samples A-14 and A-15 (see pp. 18 and 20). Comparison with samples A-14 and A-15 is made not on the basis of soak time, but rather between samples having measurable axial ^{65}Zn concentration gradients. In other words, earth-tested samples with axial ^{65}Zn concentration gradients, somewhat similar to that observed for sample A-6, demonstrated much steeper radial gradients. These observations give further support to the theory that convective mixing had little effect on the ^{65}Zn movement in the Skylab samples.

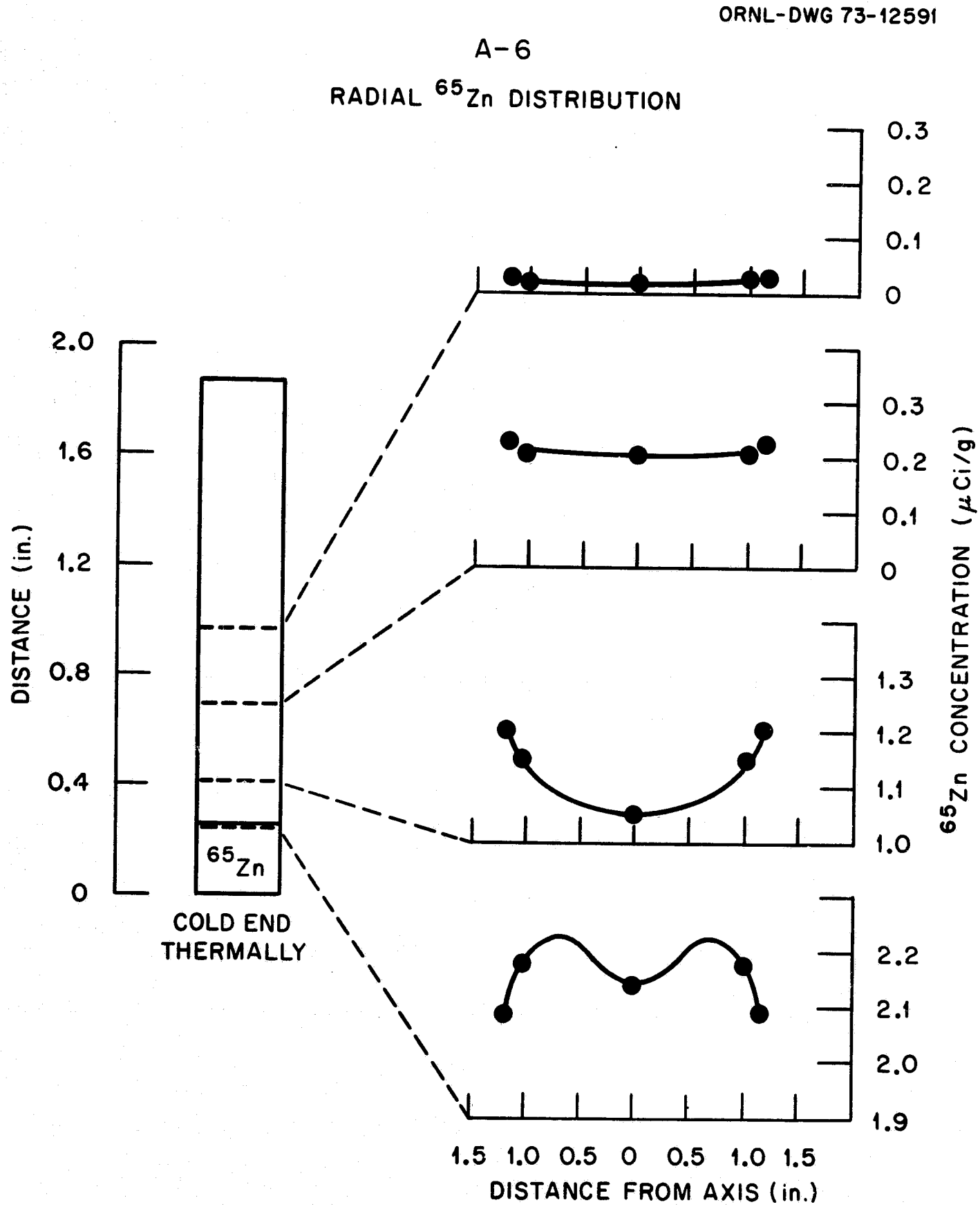

Fig. 24. Zinc-65 Radial Concentration Gradient in Sample A-6.

Skylab Sample A-7

Figure 25 shows the ^{65}Zn concentration gradient measured along the length of Skylab sample A-7. This sample was oriented with the ^{65}Zn-labeled pellet at the hot end of the gradient furnace and was subjected to a 1-hr soak time at the appropriate temperature gradient. Again a strikingly smooth ^{65}Zn concentration gradient was observed, with little or no scatter of data points, that extended to about the midpoint of the sample. In contrast, ^{65}Zn had moved across a similar sample melted on earth (see results for A-1, p. 24) so rapidly in the same length of time that a straight horizontal line on a concentration-distance plot was observed. Comparison of these results illustrates that convection forces were dominant in ^{65}Zn transport in liquid zinc in earth-bound tests, while diffusion was the principal mechanism during the melting experiment on Skylab. Intensity measurements made on selected sections to determine the radial distribution of ^{65}Zn in sample A-7 are plotted in Fig. 26. As noted for sample A-6, the radial ^{65}Zn distributions were radially more uniform in regions of low ^{65}Zn concentration and showed noticeable variations near the outer surfaces in regions of close proximity to the ^{65}Zn-labeled pellet.

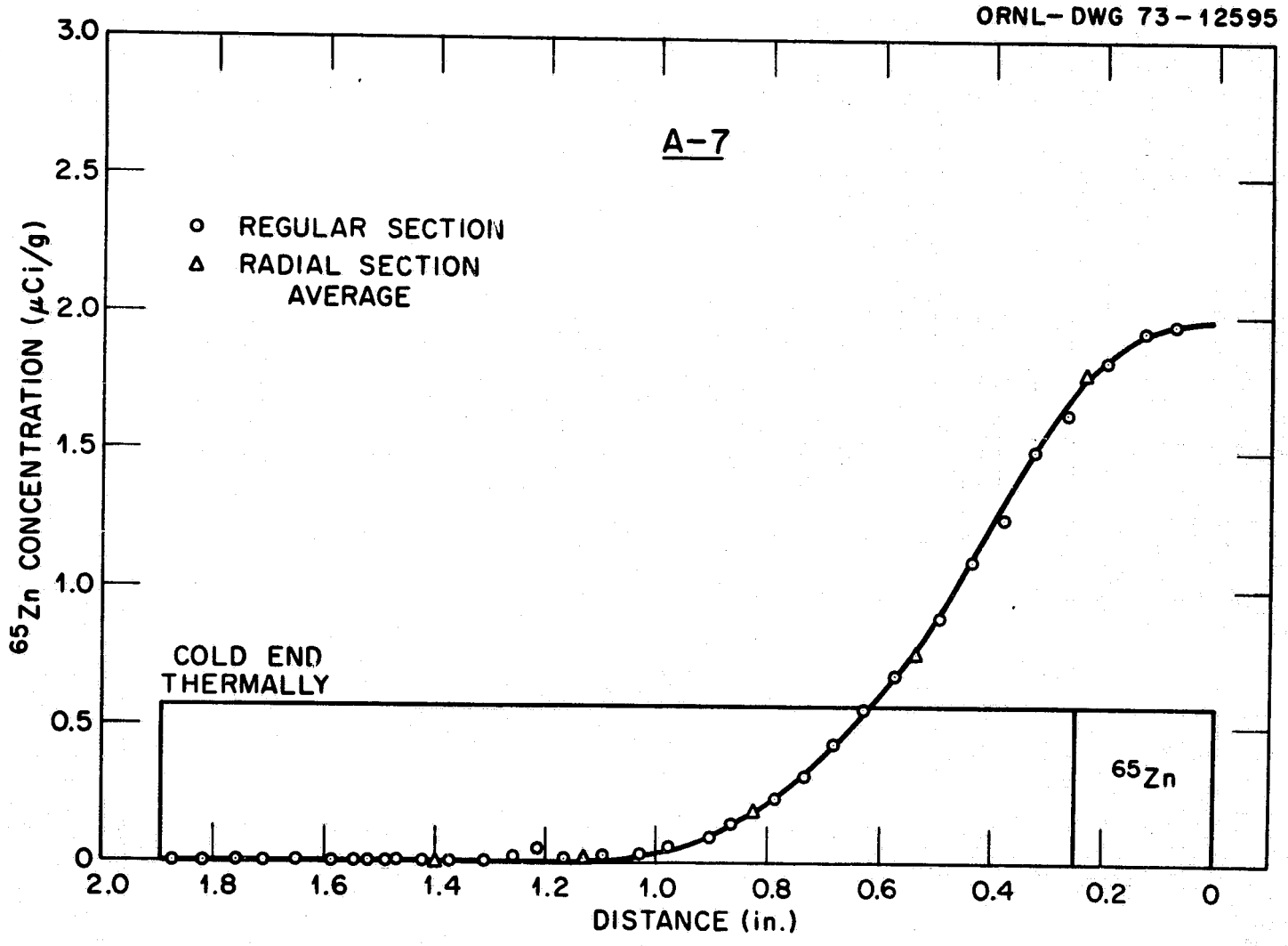

Fig. 25. Zinc-65 Axial Concentration Gradient in Sample A-7.

Radial distribution of ^{65}Zn in sample A-7 was not quite as uniform as the comparable ground-test sample A-1 (see pp. 24, 46, and 47), but again, convective mixing helped produce a virtually homogeneous ^{65}Zn distribution in earth samples within the 1-hr thermal soak time.

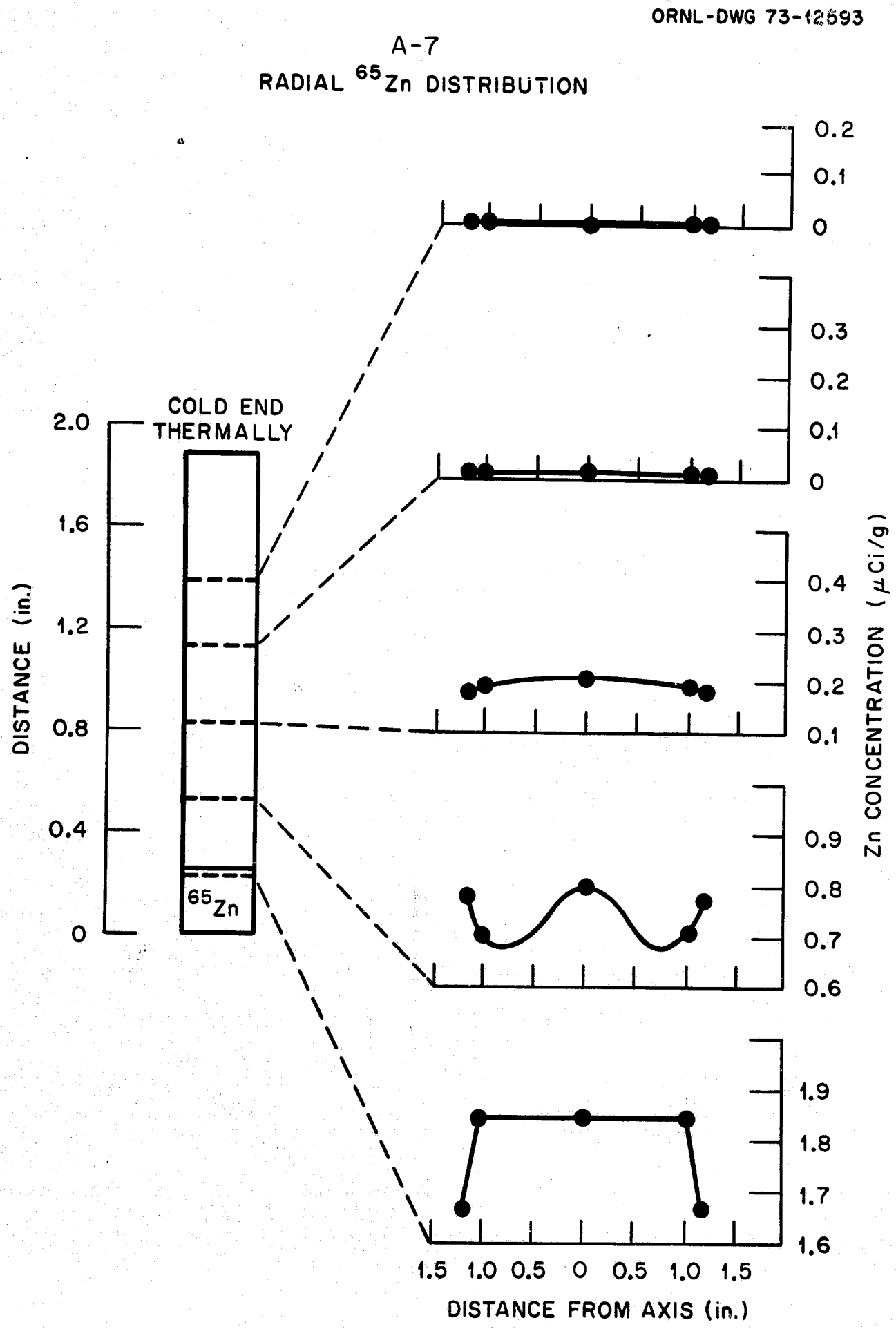

Fig. 26. Zinc-65 Radial Concentration Gradient in Sample A-7.

Skylab Sample B-5

The ^{65}Zn concentration gradient in the axial direction measured for sample B-5 is given in Fig. 27. This sample was held in the thermal gradient for a 1-hr soak period. Since sample B-5 was fabricated with the ^{65}Zn-labeled pellet in the center, diffusion of ^{65}Zn in the melt occurred in both directions from the midpoint. However, only slightly more ^{65}Zn was transported towards the thermally hotter end of the sample as compared with movement toward the colder end. Some scatter of data can be noted in Fig. 27 in the region of the ^{65}Zn-labeled pellet and along the portion of the sample nearest the cooler zone of the furnace. However, this scatter of data points is not sufficient to alter the ^{65}Zn distribution curve. Comparison of data in Fig. 27 with that obtained for sample B-13, which showed a homogeneous ^{65}Zn distribution after melting on earth (p. 24), indicated that far less ^{65}Zn movement of the liquid zinc occurred in space due to the absence of convective mixing.

The radial ^{65}Zn distribution for sample B-5 is given in Fig. 28. Again, only minor fluctuations in ^{65}Zn concentration were observed and these were located near the outer surfaces. If these radial distributions are compared to those for sample B-13 (pp. 24, 48, and 49), the ^{65}Zn concentration gradients are found to be generally similar. Since sample B-13 displayed no axial gradient, one can again infer that the ^{65}Zn diffusion (sample B-5) occurred in space without any significant convective mixing.

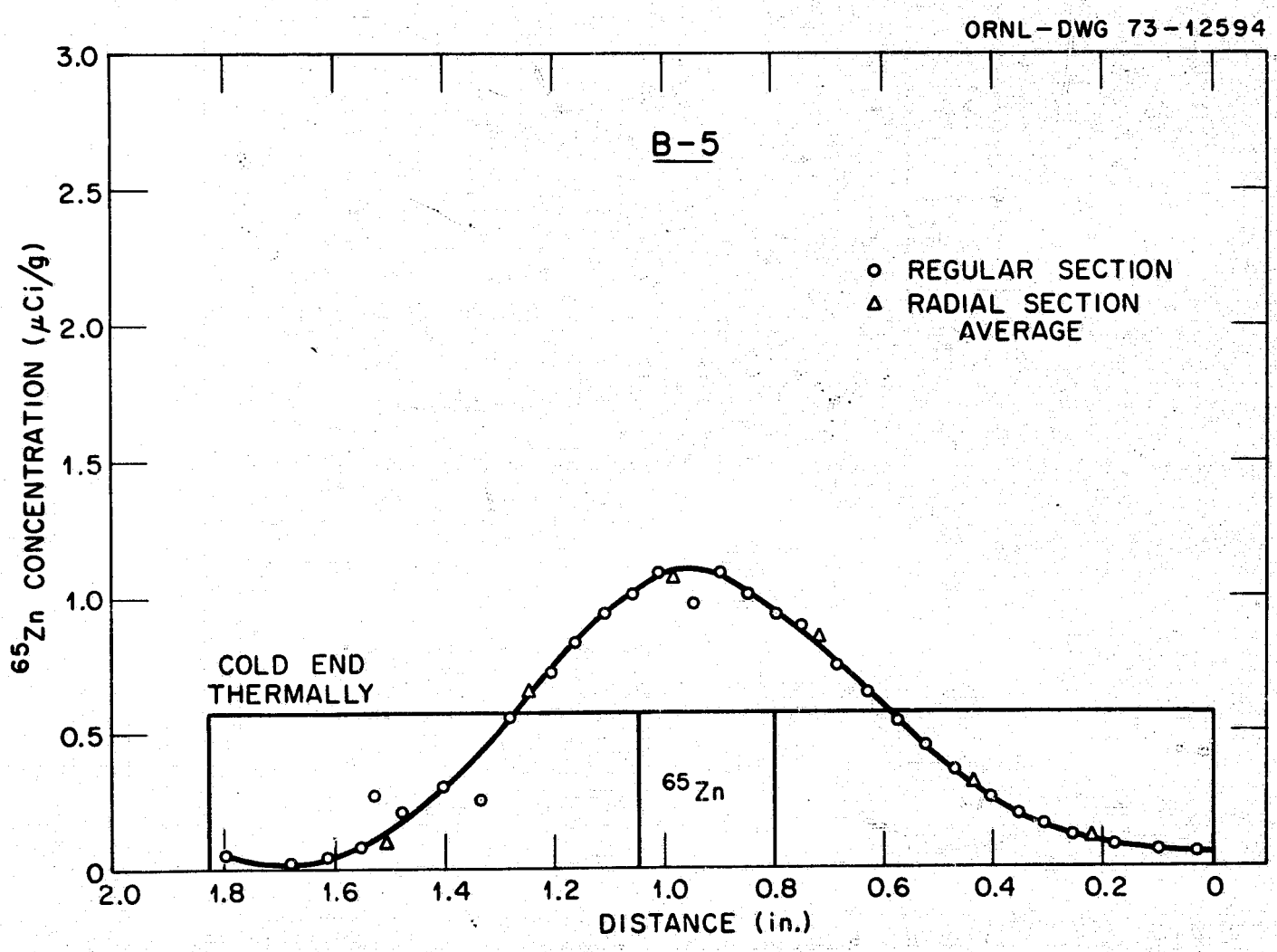

Fig. 27. Zinc-65 Axial Concentration Gradient in Sample B-5.

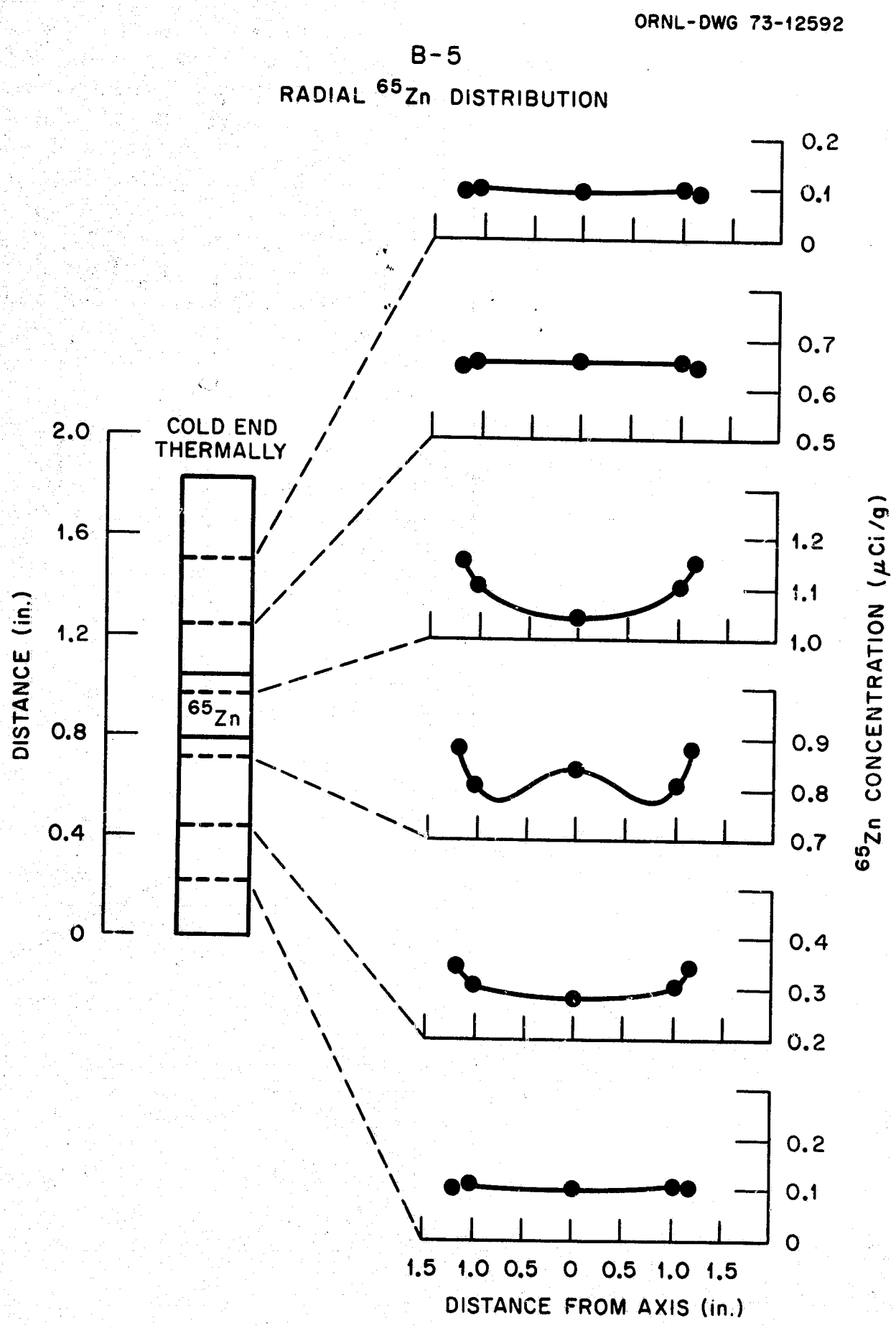

Fig. 28. Zinc-65 Radial Concentration Gradient in Sample B-5.

CONCLUSIONS

1. The Skylab samples A-6, A-7, and B-5 had unique wrinkled surfaces after melting in space (as compared with those melted in a unit gravitational field) which may have been caused by solidification-shrinkage and/or surface perturbations induced by the samples contacting the carbon liner walls of the tantalum capsule.

2. Samples melted and solidified in unit gravity and in near-zero gravity environments had small weight losses that were probably the result of some zinc vaporization during the melting and thermal soak periods of the experiments.

3. The length and diameter of the Skylab samples were little changed after melting in space, whereas gravity affected the final dimensions of the zinc samples melted on earth.

4. A 1-hr soak time in the prescribed thermal gradient produced sharp axial ^{65}Zn concentration gradients in samples melted in space and nearly homogeneous ^{65}Zn distribution in samples melted on earth. The marked decrease in ^{65}Zn movement in liquid zinc in the near-zero gravity environment was apparently caused by the absence of gravity-induced convective mixing. The relatively uniform radial ^{65}Zn distribution observed in the Skylab samples also indicates that convective mixing was negligible in space.

5. Radioactive isotopes can be successfully used for experiments in space to study liquid metal diffusion.

ACKNOWLEDGMENTS

The authors wish to commend T. R. Rice for the precision sectioning of zinc samples and J. R. Gibson for the excellent engineering support for which he was responsible. We also recognize the important support of J. S. Eldridge, J. Northcutt, and B. C. Leslie for radioactive counting and autoradiography. Special thanks to R. E. Reed for helpful discussion concerning the "wrinkled" surfaces of the Skylab samples.

APPENDIX A

Materials Analyses

I. Zinc

Vendor: Ventron Corporation, Alfa Products
Analysis: ORNL - Spectrographic

Element	Amount (ppm)	Element	Amount (ppm)
Al	0.3	P	<0.05
B	<0.05	Pb	<0.7
Ba	<0.05	Si	<0.9
Ca	<0.2	Sn	<0.05
Cr	<0.1	Ta	3.0
Cu	<0.5	Ti	<0.1
Fe	0.1	W	<0.1
K	<0.05	Cl	<0.1
Li	<0.05	*C	42
Mg	<0.1	*N	<1
Mn	<0.1	*O	46
Mo	<0.05	*S	22
Na	<0.05	Zn	Balance
Ni	<0.2		

*By vacuum fusion.

II. Carbon

Vendor: Union Carbide
Analysis: ORNL - Spectrographic

Element	Amount (ppm)	Element	Amount (ppm)
Al	7	Ni	<0.8
B	1	P	3
Ba	30	Rb	1
Ca	3000	Si	140
Cr	4	Sr	70
Cu	0.8	V	0.4
Fe	5	Zn	<20
K	10	S	<20
Mg	2	C	Balance

Appendix A (cont'd)

III. Tantalum Tubing (3/8-in. o.d. x 0.020 in. wall)

Vendor: Fansteel Metals
Analysis: Vendor

Element	Amount (ppm)	Element	Amount (ppm)
C	12	Mn	<10
O	43	Ca	<10
N	16	Al	<10
H	<5	Cu	<10
W	100	Sn	<10
Cb	230	Cr	<10
Zr	<10	V	<10
Mo	<10	Co	<10
Ti	<10	Mg	<10
Fe	<10	Pb	<10
Ni	<10	Ta	Balance
Si	<10		

IV. Tantalum Bar (3/8-in. diam)

Vendor: Teledyne - Wah Chang Albany
Ingot Analysis: By Vendor - Heat No. G00503

Element	Top (ppm)	Bottom (ppm)	Element	Top (ppm)	Bottom (ppm)
Al	<20	<20	N	22	42
C	<30	30	Ni	<10	<10
Cb	649	614	O	<50	<50
Cr	<10	<10	Si	<10	17
Cu	4	5	Ti	<10	<10
Fe	<15	<15	V	<10	<10
H	< 5	< 5	W	40	33
Mo	50	40	Zr	<50	<50
Co	< 5	< 5	Ta	Balance	Balance

(o) - outer
(i) - inner

APPENDIX B-1

A-2 Sectioning Data

Sample No.	Sample Wt (g)	Activity (μCi)	^{65}Zn Conc. (μCi/g)	Position From Cold End (in.)
A2-1	0.3168	0.47	1.48	0.021
2 (o)	0.0887	0.13	1.47	0.032 (o)
3 (i)	0.0943	0.14	1.48	0.032 (i)
4	0.3015	0.44	1.46	0.095
5	0.2381	0.35	1.47	0.132
6	0.2433	0.35	1.44	0.161
7	0.2675	0.39	1.46	0.202
8	0.1029	0.15	1.46	0.250 (o)
9	0.1710	0.25	1.46	0.250 (i)
10	0.2632	0.39	1.48	0.242
11	0.3649	0.53	1.45	0.350
12	0.6337	0.90	1.42	0.440
13	0.3578	0.52	1.45	0.472
14	0.3066	0.45	1.47	0.350
15	0.2272	0.33	1.45	0.472
16	0.3432	0.50	1.46	0.919
17	0.2821	0.42	1.49	0.872
18	0.3073	0.44	1.43	0.828
19	0.3357	0.49	1.46	0.777
20	0.2946	0.44	1.49	0.726
21	0.4972	0.71	1.43	0.682
22	0.2953	0.43	1.46	1.059
23	0.6707	0.94	1.40	1.168
24	0.4465	0.65	1.46	0.872
25	0.2041	0.29	1.42	1.059
26	0.8927	1.22	1.37	1.003
27	0.2545	0.36	1.41	1.018
28	0.1184	0.17	1.44	1.003
29	0.2291	0.33	1.44	1.018
30	0.2223	0.32	1.44	1.653
31	0.2185	0.32	1.46	1.608
32	0.3434	0.50	1.46	1.563
33	0.3006	0.43	1.43	1.518
34	0.1306	0.19	1.45	1.481 (o)
35	0.1532	0.22	1.44	1.481 (i)
36	0.3017	0.44	1.46	1.441
37	0.3501	0.51	1.46	1.388
38	0.6874	0.99	1.44	1.298
11A-6	0.3349	0.55	1.64	1.663
11A-7	0.2379	0.345	1.45	0.015
Total	12.4295	18.00		

APPENDIX B-2

A-3 Sectioning Data

(o) - outer
(i) - inner

Sample No.	Sample Wt. (g)	Activity (μCi)	^{65}Zn Conc. (μCi/g)	Position From Cold End (in.)
C-1	0.1292	0.19	1.47	1.670
2	0.1331	0.19	1.43	1.642
3	0.3151	0.47	1.49	1.642
4	0.1871	0.28	1.50	1.611
5	0.2041	0.30	1.47	1.573
6 (o)	0.0537	0.08	1.49	1.563
7 (i)	0.0784	0.11	1.40	1.563
8	0.1746	0.26	1.49	1.543
9	0.1850	0.27	1.46	1.511
10	0.1685	0.25	1.48	1.384
11	0.2510	0.37	1.47	1.222
12	0.4336	0.64	1.48	1.281
13	0.2953	0.44	1.49	1.181
14 (o)	0.0749	0.11	1.47	1.157
15 (i)	0.0810	0.12	1.48	1.157
16	0.2992	0.44	1.47	1.126
17	0.2149	0.32	1.49	1.089
18	0.2542	0.38	1.49	1.049
19	0.2599	0.39	1.50	1.006
20	0.1522	0.22	1.46	0.967
21	0.2527	0.37	1.46	0.926
22	0.2640	0.39	1.48	0.884
23	0.2378	0.35	1.47	0.847
24	0.2596	0.38	1.46	0.802
11A-19	0.6956	1.0	1.44	0.046
20	0.3665	0.55	1.50	0.108
21	0.3021	0.45	1.49	0.759
22	0.2647	0.39	1.47	0.716
23	0.2888	0.43	1.49	0.674
24	0.2818	0.42	1.49	0.630
25 (o)	0.0409	0.059	1.44	0.600
26 (i)	0.0790	0.11	1.39	0.600
27	0.2736	0.41	1.50	0.568
28	0.2719	0.40	1.47	0.524
29	0.3420	0.51	1.49	0.479
30	0.3156	0.47	1.49	0.433
31 (o)	0.1312	0.19	1.45	0.390
32 (i)	0.1050	0.16	1.53	0.390
33	0.2733	0.41	1.50	0.353
34	0.2490	0.37	1.49	0.300
35	0.2617	0.39	1.49	0.272
36	0.1351	0.20	1.48	0.240
37	0.1500	0.22	1.47	0.240
38	0.3006	0.45	1.50	0.197
39	0.2373	0.35	1.47	0.160
Total	10.324	15.26		

APPENDIX B-3

A-13 Sectioning Data

(o) - outer
(i) - inner

Sample No.	Sample Wt (g)	Activity (μCi)	^{65}Zn Conc. (μCi/g)	Position From Cold End (in.)
BA-1	0.3461	0.439	1.27	1.620
2 (o)	0.1222	0.157	1.28	1.567
3 (i)	0.1727	0.220	1.27	1.567
4	0.3159	0.408	1.29	1.535
5	0.3129	0.396	1.27	1.493
6	0.2997	0.382	1.27	1.453
7	0.2560	0.329	1.29	1.412
8	0.2937	0.380	1.29	1.370
9	0.3300	0.416	1.26	1.329
10	0.2654	0.334	1.26	1.288
11	0.3992	0.500	1.25	1.245
12	0.3344	0.427	1.28	1.204
13	0.3034	0.383	1.26	1.163
14	0.3351	0.427	1.27	1.222
15	0.3319	0.420	1.27	1.081
16	0.3335	0.422	1.27	1.038
17	0.3318	0.424	1.28	0.996
18	0.3090	0.395	1.28	0.953
19	0.3276	0.415	1.27	0.910
20	0.3107	0.394	1.27	0.867
21	0.3200	0.407	1.27	0.825
22	0.3114	0.394	1.27	0.783
23	0.2866	0.364	1.27	0.741
24	0.2210	0.276	1.25	0.697
25	0.2697	0.343	1.27	0.651
26	0.1911	0.232	1.21	0.605
27	0.2359	0.298	1.26	0.559
28	0.7639	0.943	1.23	0.514
29	0.2581	0.332	1.29	0.461
30 (o)	0.0697	0.089	1.28	0.439
31 (i)	0.0980	0.124	1.27	0.439
32	0.2402	0.303	1.26	0.411
33	0.3088	0.388	1.26	0.373
34	0.3767	0.473	1.26	0.329
35	0.2926	0.373	1.27	0.287
36	0.3037	0.386	1.27	0.248
37 (o)	0.0950	0.119	1.25	0.214
38 (i)	0.0991	0.124	1.25	0.214
39	0.2712	0.341	1.26	0.185
40	0.2860	0.362	1.27	0.142
41	0.2394	0.302	1.26	0.025
42	0.3258	0.409	1.26	0.060
43	0.3958	0.495	1.25	0.105
11A-11	0.1101	0.12	1.09	1.672
11A-12	0.0668	0.085	1.27	0.012
Total	12.470	15.77		

APPENDIX B-4

A-14 Sectioning Data

(o) - outer
(i) - inner

Sample No.	Sample Wt (g)	Activity (μCi)	^{65}Zn Conc. (μCi/g)	Position From Cold End (in.)
A14-1	0.1267	0.00624	0.049	1.741
2	0.2363	0.0243	0.103	1.692
3	0.2695	0.0333	0.124	1.657
4	0.2626	0.0327	0.125	1.619
5	0.2531	0.0325	0.128	1.582
6	0.2400	0.0321	0.134	1.546
7	0.3103	0.0448	0.144	1.509
8	0.2883	0.0448	0.155	1.470
9	0.2958	0.0475	0.160	1.429
10	0.3517	0.0594	0.169	1.388
11	0.2346	0.0412	0.176	1.346
12	0.3083	0.0579	0.188	1.306
13	0.3198	0.0670	0.210	1.266
14	0.3308	0.0844	0.255	1.225
15	0.2169	0.0636	0.293	1.184
16	0.3126	0.103	0.329	1.142
17	0.2976	0.113	0.380	1.097
18	0.3276	0.144	0.440	1.053
19	0.3754	0.185	0.493	1.008
20	0.3170	0.163	0.514	0.964
21	-			-
22	0.3353	0.175	0.522	0.920
23	0.2479	0.144	0.580	0.879
24	0.2885	0.20	0.693	0.842
25	0.3071	0.26	0.847	0.805
26	0.2580	0.28	1.085	0.772
27 (o)[1]	0.0944	0.05	0.530	0.740
28 (i)[1]	0.1312	0.23	1.753	0.740
29	0.3809	0.54	1.42	0.703
30	0.2955	0.46	1.56	0.658
31	0.2875	1.10	3.83	0.017
32	0.2691	0.88	3.27	0.042
33	0.3274	1.05	3.21	0.080
34	0.3066	1.0	3.26	0.120
35	0.3780	1.21	3.20	0.162
36	0.3381	1.05	3.11	0.210
37	0.3178	0.535	1.68	0.616
38	0.3087	0.58	1.88	0.576
39 (o)[2]	0.1135	0.10	0.88	0.540
40 (i)[2]	0.1484	0.40	2.70	0.540
41	0.3040	0.60	1.97	0.504
42	0.2960	0.59	1.99	0.464
43	0.3154	0.69	2.19	0.424
44	0.3077	0.78	2.53	0.384
45 (o)[3]	0.0955	0.17	1.78	0.350
46 (i)[3]	0.1617	0.555	3.43	0.350
47	0.2594	0.77	2.97	0.321
48	0.4284	1.25	2.92	0.271
Total	12.977	17.029		

[1]Concentration of outer and inner section (μCi/g): 1.24; [2]Concentration of outer and inner section (μCi/g): 1.91; [3]Concentration of outer and inner section (μCi/g): 2.82.

(o) - outer
(m) - middle
(i) - inner

APPENDIX B-5

A-15 Sectioning Data

Sample No.	Sample Wt. (g)	Activity (μCi)	^{65}Zn Conc. (μCi/g)	omi Avg. (μCi/g)	Position From Hot End (in.)
N-1	0.1460	0.078	0.534		1.720
2	0.2885	0.138	0.478		1.680
3	0.3238	0.168	0.519		1.639
4 (o)	0.0410	0.020	0.488		1.611
5 (m)	0.0467	0.026	0.557	0.597	1.611
6 (i)	0.0412	0.031	0.752		1.611
7	0.3278	0.225	0.686		1.582
8	0.3333	0.247	0.741		1.541
9	0.3270	0.252	0.770		1.500
10	0.2999	0.235	0.783		1.459
11	0.2714	0.215	0.792		1.415
12	0.2525	0.206	0.815		1.372
13	0.2720	0.227	0.834		1.330
14	0.2896	0.264	0.911		1.286
15	0.2986	0.300	1.004		1.243
16	0.3109	0.530	1.704		0.692
17	0.4834	0.528	1.092		1.195
18 (o)	0.0359	0.033	0.919		1.160
19 (m)	0.0411	0.038	0.924	1.032	1.160
20 (i)	0.0557	0.066	1.184		1.160
21	0.3312	0.364	1.099		1.131
22	0.3389	0.395	1.165		1.089
23	0.3405	0.409	1.201		1.047
24	0.3393	0.410	1.208		1.005
25	0.3279	0.401	1.222		0.962
26 (o)	0.0376	0.044	1.170		0.933
27 (m)	0.0429	0.051	1.188	1.217	0.933
28 (i)	0.0427	0.055	1.288		0.933
29	0.3625	0.450	1.241		0.905
30	0.2677	0.345	1.288		0.865
31	0.3089	0.420	1.359		0.826
32	0.3090	0.462	1.495		0.787
33 (o)	0.0471	0.071	1.507		0.759
34 (m)	0.0422	0.065	1.540	1.554	0.759
35 (i)	0.0349	0.057	1.633		0.759
36	0.3281	0.541	1.648		0.732
37	0.3109	0.538	1.730		0.652
38	0.2899	0.481	1.659		0.612
39	0.3356	0.547	1.629		0.571
40 (o)	0.0366	0.059	1.612		0.544
41 (m)	0.0403	0.065	1.612	1.582	0.544
42 (i)	0.0407	0.062	1.523		0.544
43	0.3325	0.549	1.651		0.514

Appendix B-5 (Cont'd)

Sample No.	Sample Wt (g)	Activity (μCi)	^{65}Zn Conc. (μCi/g)	omi Avg. (μCi/g)	Position From Hot End (in.)
N-44	0.3566	0.583	1.634		0.471
45	0.3308	0.565	1.707		0.428
46	0.3319	0.563	1.696		0.385
47	0.3685	0.626	1.698		0.342
48 (o)	0.0448	0.083	1.852		0.313
49 (m)	0.0431	0.067	1.554	1.639	0.313
50 (i)	0.0390	0.058	1.487		0.313
51	0.3268	0.596	1.823		0.020
52 (o)	0.0390	0.066	1.692		0.049
53 (m)	0.0438	0.059	1.347	1.419	0.049
54 (i)	0.0342	0.041	1.198		0.049
55	0.3225	0.503	1.559		0.284
56	0.3217	0.499	1.551		0.243
57	0.3163	0.483	1.527		0.202
58	0.2821	0.420	1.488		0.164
59	0.2554	0.363	1.421		0.130
60	0.4629	0.629	1.358		0.084
Total	13.2536	16.872			

(o) - outer
(m) - middle
(i) - inner

APPENDIX B-6

A-0 Sectioning Data

Sample No.	Sample Wt. (g)	Activity (μCi)	^{65}Zn Conc. (μCi/g)	omi Avg. (μCi/g)	Position From Hot End (in.)
K-1	0.5282	0.470	0.889		1.660
2	0.2518	0.230	0.913		1.620
3	0.2879	0.260	0.903		1.582
4	0.2819	0.254	0.901		1.540
5	0.2595	0.233	0.897		1.495
6	0.2292	0.206	0.898		1.451
7	0.2143	0.190	0.886		1.451
8	0.2833	0.260	0.917		1.410
9	0.3010	0.271	0.900		1.370
10	0.3166	0.285	0.900		1.330
11	0.2543	0.230	0.904		1.294
12 (o)	0.0330	0.030	0.909		1.270
13 (m)	0.0406	0.040	0.985	0.927	1.270
14 (i)	0.0347	0.031	0.893		1.270
15	0.3099	0.280	0.903		1.241
16	0.2864	0.260	0.907		1.20)
17	0.2739	0.245	0.894		1.161
18	0.2479	0.230	0.927		1.131
19	0.1919	0.172	0.896		1.100
20 (o)	0.0308	0.030	0.974		1.080
21 (m)	0.0360	0.033	0.916	0.902	1.080
22 (i)	0.0370	0.033	0.891		1.080
23	0.2664	0.240	0.900		1.051
24	0.2963	0.270	0.911		1.012
25	0.2898	0.260	0.897		0.973
26	0.2928	0.262	0.894		0.933
27	0.3018	0.270	0.894		0.891
28 (o)	0.0248	0.023	0.927		0.862
29 (m)	0.0507	0.050	0.986	0.970	0.862
30 (i)	0.0401	0.040	0.997		0.862
31	0.3074	0.274	0.891		0.834
32	0.2779	0.250	0.899		0.800
33	0.1128	0.100	0.886		0.770
34	0.2037	0.181	0.888		0.730
35	0.2135	0.192	0.899		0.690
36	0.2393	0.212	0.885		0.650
37	0.2579	0.230	0.891		0.610
38	0.3460	0.310	0.895		0.562
39	0.2691	0.241	0.895		0.522
40	0.3914	0.340	0.868		0.650
41	0.2844	0.251	0.882		0.490
42	0.2808	2.81	10.007		0.020
43	0.2768	2.72	9.826		0.060
44	0.2776	1.52	5.475		0.092
45	0.3009	0.273	0.907		0.130

Appendix B-6 (Cont'd)

Sample No.	Sample Wt (g)	Activity (μCi)	^{65}Zn Conc. (μCi/g)	omi Avg. (μCi/g)	Position From Hot End (in.)
K-46 (o)	0.0298	0.030	1.006		0.155
47 (m)	0.0446	0.040	0.896	0.938	0.155
48 (i)	0.0535	0.050	0.934		0.155
49	0.3289	0.300	0.912		0.181
50	0.2525	0.230	0.910		0.220
51	0.3189	0.290	0.909		0.260
52	0.3129	0.283	0.904		0.300
53	0.3294	0.293	0.889		0.340
54 (o)	0.0207	0.020	0.966		0.365
55 (m)	0.0412	0.040	0.970	0.931	0.365
56 (i)	0.0369	0.032	0.867		0.365
57	0.2301	0.210	0.912		0.390
58	0.4856	0.424	0.873		0.434
Total	12.8173	17.834			

(o) - outer
(m) - middle
(i) - inner

APPENDIX B-7

A-1 Sectioning Data

Sample No.	Sample Wt (g)	Activity (μCi)	^{65}Zn Conc. (μCi/g)	omi Avg. (μCi/g)	Position From Hot End (in.)
L-1	0.3231	0.400	1.238		1.663
2	0.2299	0.284	1.235		1.620
3	0.1687	0.199	1.179		1.620
4	0.3292	0.401	1.218		1.578
5	0.4079	0.493	1.208		1.578
6	0.1982	0.243	1.226		1.514
7	0.3348	0.402	1.200		1.469
8	0.2944	0.357	1.212		1.421
9 (o)	0.0252	0.031	1.230		1.393
10 (m)	0.0332	0.041	1.234	1.227	1.393
11 (i)	0.0427	0.052	1.217		1.393
12	0.2452	0.300	1.223		1.369
13	0.3197	0.391	1.223		1.331
14	0.3601	0.441	1.224		1.287
15	0.2751	0.333	1.210		1.247
16	0.3368	0.406	1.205		1.210
17 (o)	0.0290	0.035	1.206		1.182
18 (m)	0.0482	0.058	1.203	1.214	1.182
19 (i)	0.0437	0.054	1.235		1.182
20	0.3148	0.385	1.222		1.155
21	0.3068	0.372	1.212		1.114
22	0.3187	0.388	1.217		1.073
23	0.3056	0.376	1.230		1.032
24	0.3034	0.370	1.219		0.990
25 (o)	0.0320	0.037	1.156		0.962
26 (m)	0.0422	0.049	1.161	1.214	0.962
27 (i)	0.0314	0.037	1.178		0.962
28	0.2964	0.364	1.228		0.935
29	0.3009	0.370	1.229		0.896
30	0.2739	0.333	1.215		0.853
31	0.3685	0.451	1.223		0.808
32	0.2973	0.363	1.220		0.767
33 (o)	0.0334	0.038	1.137		0.739
34 (m)	0.0451	0.051	1.130	1.120	0.739
35 (i)	0.0402	0.044	1.094		0.739
36	0.2972	0.364	1.224		0.710
37	0.3119	0.376	1.205		0.658
38	0.2925	0.358	1.223		0.626
39	0.3299	0.405	1.227		0.586
40	0.3109	0.377	1.212		0.543
41	0.2806	0.341	1.215		0.495
42	0.1701	0.199	1.169		0.495
43	0.3879	0.477	1.229		0.438
44 (o)	0.0341	0.040	1.173		0.400
45 (m)	0.0444	0.053	1.193	1.19	0.400
46 (i)	0.0423	0.051	1.205		0.400

Appendix B-7 (Cont'd)

Sample No.	Sample Wt (g)	Activity (μCi)	^{65}Zn Conc. (μCi/g)	omi Avg. (μCi/g)	Position From Hot End (in.)
L-47	0.3020	0.364	1.205		0.372
48	0.3019	0.368	1.218		0.332
49	0.3383	0.419	1.238		0.291
50	0.3182	0.384	1.206		0.253
51	0.3207	0.385	1.200		0.207
A2-40 (o)	0.0332	0.037	1.114		0.178
41 (m)	0.0382	0.045	1.178	1.131	0.178
42 (i)	0.0418	0.046	1.100		0.178
43	0.3636	0.322	0.885		0.159
44	0.6913	0.821	1.187		0.093
45	0.3901	0.476	1.220		0.024
Total	12.9968	15.657			

(o) - outer
(m) - middle
(i) - inner

APPENDIX B-8

B-13 Sectioning Data

Sample No.	Sample Wt (g)	Activity (μCi)	^{65}Zn Conc. (μCi/g)	omi Avg. (μCi/g)	Position From Hot End (in.)
M-1	0.1855	0.210	1.132		1.629
2	0.2533	0.288	1.136		1.595
3	0.2910	0.336	1.154		1.561
4	0.2732	0.311	1.138		1.527
5	0.3890	0.330	0.848		1.493
6 (o)	0.0491	0.056	1.140		1.467
7 (m)	0.0467	0.054	1.156	1.145	1.467
8 (i)	0.0386	0.044	1.139		1.467
9	0.3055	0.348	1.139		1.403
10	0.2846	0.324	1.138		1.440
11	0.3242	0.369	1.138		1.363
12	0.2952	0.335	1.134		1.320
13	0.3695	0.424	1.147		1.277
14 (o)	0.0451	0.050	1.108		1.247
15 (m)	0.0480	0.053	1.104	1.061	1.247
16 (i)	0.0474	0.049	1.033		1.247
17	0.3219	0.373	1.158		1.218
18	0.3144	0.355	1.129		1.175
19	0.3353	0.381	1.136		1.135
20	0.3390	0.387	1.141		1.094
21	0.4179	0.477	1.141		1.046
22	0.3316	0.381	1.148		1.098
23 (o)	0.0476	0.053	1.113		0.969
24 (m)	0.0480	0.052	1.083	1.078	0.969
25 (i)	0.0385	0.040	1.038		0.969
26	0.3443	0.392	1.138		0.939
27	0.2749	0.314	1.142		0.898
28	0.3289	0.375	1.140		0.857
29	0.3530	0.400	1.133		0.817
30	0.3474	0.402	1.157		0.774
31 (o)	0.0492	0.054	1.097		0.744
32 (m)	0.0402	0.046	1.144	1.112	0.744
33	0.2785	0.316	1.134		0.714
34	0.3362	0.383	1.139		0.671
35 (i)	0.0356	0.039	1.095	1.112	0.744
36	0.3818	0.438	1.147		0.628
37	0.4116	0.468	1.137		0.585
38	0.2751	0.313	1.137		0.542
39 (o)	0.0507	0.059	1.163		0.513
40 (m)	0.0406	0.045	1.108	1.101	0.513
41 (i)	0.0378	0.039	1.031		0.513
42	0.3377	0.385	1.140		0.484
43	0.3220	0.368	1.142		0.443
44	0.3079	0.352	1.143		0.402
45	0.3208	0.366	1.140		0.361

Appendix B-8 (Cont'd)

Sample No.	Sample Wt (g)	Activity (μCi)	^{65}Zn Conc. (μCi/g)	omi Avg. (μCi/g)	Position From Hot End (in.)
M-46	0.3067	0.349	1.137		0.321
47 (o)	0.0398	0.044	1.105		0.293
48 (m)	0.0524	0.056	1.068	1.077	0.293
49 (i)	0.0378	0.040	1.058		0.293
50	0.3174	0.359	1.131		0.264
51	0.3168	0.356	1.123		0.223
52	0.3360	0.383	1.139		0.183
53	0.3099	0.348	1.122		0.143
54 (o)	0.0596	0.066	1.107		0.115
55 (m)	0.0599	0.064	1.068	1.093	0.115
56 (i)	0.0435	0.048	1.103		0.115
57	0.2743	0.311	1.133		0.087
58	0.5116	0.565	1.104		0.033
Total	12.9800	14.623			

(o) - outer
(m) - middle
(i) - inner

APPENDIX C

A6 Sectioning Data

Sample No.	Sample Wt (g)	Activity (μCi)	^{65}Zn Conc. (μCi/g)	omi Avg. (μCi/g)	Position From Thermal Cold End (in.)
A6-1	0.2308	0.000006	0.00003		1.855
-2	0.3159				1.816
-3	0.2809				1.774
-4	0.4362				1.729
-5	0.2433	0.00007	0.0003		1.684
-6	0.0348				1.659 (o)
-7	0.0574				1.659 (i)
-8	0.2267				1.630
-9	0.2458				1.588
-10	0.2338	0	0		1.568
-11	0.2530				1.506
-12	0.2864				1.463
-13	0.0627				1.434 (o)
-14	0.0380				1.434 (i)
-15	0.2642	0.00004	0.0002		1.405
-16	0.2730				1.362
-17	0.2772				1.319
-18	0.3447				1.276
-19	0.2948				1.232
-20	0.0487	0.0001	0.021		1.196 (o)
-21	0.0787				1.196 (m)
-22	0.0647				1.196 (i)
-23	0.2898				1.162
-24	0.2995				1.121
-25	0.2998	0.0019	0.006		1.078
-26	0.2950	0.0029	0.010		1.037
-27	0.2969	0.0047	0.016		0.996
-28	0.0351	0.0008	0.023		0.969 (o)
-29	0.0414	0.0009	0.022	0.021	0.969 (m)
-30	0.0350	0.0006	0.017		0.969 (i)
-31	0.3575	0.010	0.028		0.937
-32	0.3731	0.017	0.046		0.887
-33	0.4118	0.029	0.070		0.837
-34	0.3778	0.042	0.111		0.787
-35	0.3133	0.050	0.159		0.738
-36	0.0671	0.015	0.224		0.697 (o)
-37	0.0921	0.019	0.206	0.212	0.697 (m)
-38	0.0779	0.016	0.205		0.697 (i)

Appendix C (Cont'd)

Sample No.	Sample Wt (g)	Activity (μCi)	^{65}Zn Conc. (μCi/g)	omi Avg. (μCi/g)	Position From Thermal Cold End (in.)
A6-39	0.3919	0.112	0.285		0.655
-40	0.3902	0.156	0.400		0.602
-41	0.4107	0.224	0.545		0.550
-42	0.3934	0.297	0.750		0.498
-43	0.3943	0.386	0.979		0.447
-44	0.0410	0.049	1.200		0.413 (o)
-45	0.0407	0.047	1.155	1.135	0.413 (m)
-46	0.0438	0.046	1.050		0.413 (i)
-47	0.3912	0.529	1.352		0.378
-48	0.3972	0.654	1.646		0.326
-49	0.3504	0.685	1.954		0.276
-50	0.2473	0.702	2.838		0.026
-51	0.0353	0.074	2.096		0.245 (o)
-52	0.0441	0.096	2.177	2.139	0.245 (m)
-53	0.0443	0.095	2.144		0.245 (i)
-54	0.2991	0.690	2.307		0.219
-55	0.2831	0.696	2.459		0.181
-56	0.2130	0.564	2.648		0.143
-57	0.4938	1.370	2.774		0.088
Total	13.1595	7.66			

(o) - outer
(m) - middle
(i) - inner

APPENDIX D

A7 Sectioning Data

Sample No.	Sample Wt (g)	Activity (μCi)	^{65}Zn Conc. (μCi/g)	omi Avg. (μCi/g)	Position From Thermal Hot End (in.)	
A7-1	0.2573	0.003	0.001		1.871	
-2	0.2523	0.513	2.03		0.023	
-3	0.4359	0.007	0.001		1.818	
-4	0.3692	0.005	0.001		1.764	
-5	0.3970	0.003	0.001		1.710	
-6	0.4484	0.005	0.001		1.656	
-7	0.1310	<0.0001	0.001		1.547	
-8	0.3396	0.0008	0.001		1.598	
-9	0.3530	0.002	0.001		1.528	
-10	0.2383	0.002	0.001		1.471	
-11	0.2135	<0.0001	0.001		1.492	
-12	0.3424	0.005	0.001		1.422	
-13	0.0326	0.0002	0.006		1.395	(o)
-14	0.0390	<0.0001	0.003	0.004	1.395	(m)
-15	0.0503	<0.0001	0.002		1.395	(i)
-16	0.3688	0.0003	0.001		1.375	
-17	0.3610	0.0008	0.002		1.316	
-18	0.3833	0.004	0.010		1.266	
-19	0.3532	0.167	0.047		1.216	
-20	0.3721	0.004	0.011		1.166	
-21	0.0330	0.0004	0.012		1.133	(o)
-22	0.0337	0.0004	0.012	0.013	1.133	(m)
-23	0.0407	0.0006	0.015		1.133	(i)
-24	0.4315	0.009	0.021		1.097	
-25	0.4065	0.015	0.037		1.034	
-26	0.3706	0.022	0.059		0.977	
-27	0.4324	0.040	0.093		0.911	
-28	0.4165	0.061	0.138		0.866	
-29	0.0277	0.005	0.181		0.826	(o)
-30	0.0358	0.007	0.208	0.198	0.826	(m)
-31	0.0583	0.012	0.206		0.826	(i)
-32	0.3177	0.074	0.232		0.790	
-33	0.4161	0.132	0.317		0.736	
-34	0.3928	0.169	0.430		0.681	
-35	0.4074	0.229	0.562		0.631	
-36	0.3352	0.234	0.698		0.572	
-37	0.0309	0.024	0.777		0.535	(o)
-38	0.0403	0.029	0.720	0.764	0.535	(m)
-39	0.0553	0.044	0.796		0.535	(i)

Appendix D (Cont'd)

Sample No.	Sample Wt (g)	Activity (μCi)	^{65}Zn Conc. (μCi/g)	omi Avg. (μCi/g)	Position From Thermal Hot End (in.)
A7-40	0.4168	0.375	0.900		0.498
-41	0.4309	0.473	1.098		0.439
-42	0.4405	0.551	1.251		0.381
-43	0.3621	0.542	1.500		0.323
-44	0.3418	0.562	1.644		0.267
-45	0.0253	0.042	1.660		0.231 (o)
-46	0.0315	0.058	1.841	1.781	0.231 (m)
-47	0.0516	0.095	1.841		0.231 (i)
-48	0.4187	0.770	1.839		0.194
-49	0.3370	0.655	1.944		0.137
-50	0.3907	0.769	1.968		0.078
Total	13.2675	6.699			

(o) - outer
(m) - middle
(i) - inner

APPENDIX E

B5 Sectioning Data

Sample No.	Sample Wt (g)	Activity (μCi)	^{65}Zn Conc. (μCi/g)	omi Avg. (μCi/g)	Position From Thermal Hot End (in.)
B5-1	0.1871	0.010	0.053		1.800
-2	0.3081	0.016	0.052		0.029
-3	0.4124	0.014	0.034		1.682
-4	0.4280	0.021	0.049		1.619
-5	0.4566	0.035	0.077		1.556
-6	0.0320	0.003	0.094		1.517 (o)
-7	0.0276	0.003	0.109	0.098	1.517 (m)
-8	0.0332	0.003	0.090		1.517 (i)
-9	0.5130	0.136	0.265		1.534
-10	0.4624	0.096	0.208		1.470
-11	0.4944	0.149	0.301		1.408
-12	0.4729	0.120	0.254		1.345
-13	0.4742	0.264	0.557		1.284
-14	0.0387	0.025	0.646		1.248 (o)
-15	0.0364	0.024	0.659	0.653	1.248 (m)
-16	0.0351	0.023	0.655		1.248 (i)
-17	0.4025	0.290	0.720		1.215
-18	0.4056	0.336	0.828		1.600
-19	0.3830	0.357	0.932		1.113
-20	0.4060	0.413	1.017		1.064
-21	0.3687	0.402	1.090		1.011
-22	0.0414	0.048	1.159		0.979 (o)
-23	0.0332	0.037	1.114	1.107	0.979 (m)
-24	0.0430	0.045	1.047		0.979 (i)
-25	0.4071	0.402	0.987		0.948
-26	0.3892	0.425	1.092		0.899
-27	0.3822	0.398	1.041		0.849
-28	0.3019	0.296	0.928		0.799
-29	0.3572	0.316	0.885		0.749
-30	0.0318	0.028	0.880		0.716 (o)
-31	0.0358	0.029	0.810	0.843	0.716 (m)
-32	0.0370	0.031	0.838		0.716 (i)
-33	0.3834	0.285	0.743		0.681
-34	0.3895	0.250	0.642		0.628
-35	0.3860	0.208	0.539		0.576
-36	0.4092	0.182	0.445		0.522
-37	0.3819	0.137	0.359		0.469

Appendix E (Cont'd)

Sample No.	Sample Wt (g)	Activity (μCi)	^{65}Zn Conc. (μCi/g)	omi Avg. (μCi/g)	Position From Thermal Hot End (in.)
B5-38	0.0379	0.013	0.343		0.435 (o)
-39	0.0394	0.012	0.305	0.309	0.435 (m)
-40	0.0500	0.014	0.280		0.435 (i)
-41	0.3682	0.094	0.255		0.402
-42	0.3583	0.070	0.195		0.352
-43	0.3110	0.047	0.151		0.302
-44	0.3497	0.041	0.117		0.251
-45	0.0296	0.003	0.101		0.220 (o)
-46	0.0271	0.003	0.111	0.104	0.220 (m)
-47	0.0240	0.0024	0.100		0.220 (i)
-48	0.4448	0.035	0.079		0.178
-49	0.5700	0.032	0.56		0.100
Total	12.9977	6.255			